

Integrated Multi-omics Mechanism of Optimal Temperatures for *Microcystis Aeruginosa*

by

Li Liu

DKU Global Health Program
Duke University

Defense Date: April 2, 2025

Approved:

Huansheng Cao, Advisor

Chenkai Wu, Chair

Junfeng Zhang

Qian Long

Thesis submitted in partial fulfillment of the requirements for the degree of Master of
Science in the DKU Global Health Program in The Graduate School of
Duke University
2025

ABSTRACT

Integrated Multi-omics Mechanism of Optimal Temperatures for *Microcystis Aeruginosa*

by

Li Liu

DKU Global Health Program
Duke University

Defense Date: April 2, 2025

Approved:

Huansheng Cao, Advisor

Chenkai Wu, Chair

Junfeng Zhang

Qian Long

An abstract of a thesis submitted in partial fulfillment of the requirements for the degree of
Master of Science in the DKU Global Health Program in The Graduate School of
Duke University
2025

Copyright by
Li Liu
2025

Abstract

Background

Cyanobacterial blooms pose a global environmental challenge, with Lake Taihu being one of the most severely affected regions. *Microcystis aeruginosa* is the dominant cyanobacterial species responsible for these blooms in Lake Taihu. Temperature is considered a key environmental driver influencing the formation of *M. aeruginosa* blooms. However, the molecular mechanisms underlying its temperature adaptation remain unclear. Previous studies have suggested that long-chain fatty acids (MLCFAs) play a crucial role in maintaining membrane stability and regulating energy metabolism, potentially contributing to temperature adaptation. To systematically investigate the adaptive mechanisms of *M. aeruginosa* under different temperature conditions, this study employed multi-omics approaches to integrate various biological data and elucidate regulatory processes at different levels.

Methods

In this study, we first measured the growth rates of *M. aeruginosa* at different temperatures and analyzed the composition of fatty acids under each condition. Pearson correlation analysis was performed to examine the relationship between growth rate and fatty acid content, and transcriptomic data were used to explore the gene expression patterns associated with fatty acid biosynthesis. Furthermore, weighted gene co-expression network analysis (WGCNA) was applied to identify key gene modules associated with temperature adaptation, followed by Gene Ontology (GO) enrichment analysis using TopGO to infer potential biological functions. Finally, an exogenous fatty acid supplementation experiment was conducted to validate the role of specific fatty acids in promoting *M. aeruginosa* growth under low-temperature conditions.

Results

Our results showed that the growth rate of *M. aeruginosa* began to accelerate at 25°C and reached its peak at 29°C. The composition of MLCFAs varied significantly across different temperatures, and correlation analysis revealed a strong positive relationship between total fatty acid content and growth rate. Further analysis of fatty acid metabolic pathways suggested that temperature changes led to increased fatty acid consumption, affecting their intracellular accumulation. The validation experiment confirmed that the supplementation of C18:3n3(9,12,15), C20:3n6(8,11,14), and C20:3n3(11,14,17) significantly enhanced the growth rate of *M. aeruginosa* at low temperatures (15°C). Transcriptomic analysis revealed extensive transcriptional reprogramming under different temperature conditions, particularly in pathways related to fatty acid biosynthesis, energy metabolism, and stress responses. WGCNA identified key gene modules strongly associated with fatty acid metabolism, suggesting potential regulatory mechanisms involved in temperature adaptation.

Conclusion

This study provides novel insights into the molecular basis of *M. aeruginosa* temperature adaptation by elucidating the interplay between growth, fatty acid metabolism, and gene expression regulation. The findings highlight the critical role of fatty acid metabolism in temperature adaptation and reveal coordinated regulation at the gene-transcript-metabolism level in response to temperature variations. These results contribute to a deeper understanding of cyanobacterial bloom dynamics and offer valuable knowledge for developing strategies to manage *M. aeruginosa* blooms in eutrophic water bodies.

Contents

Abstract.....	iv
List of Tables	ix
List of Figures.....	x
1. Introduction	1
1.1 Cyanobacteria and Cyanobacterial Blooms	1
1.1.1 Overview of Cyanobacteria	1
1.1.2 Formation and Impacts of Cyanobacterial Blooms	2
1.2 Formation of Cyanobacterial Blooms in Lake Taihu and the Adaptation Mechanisms of <i>Microcystis aeruginosa</i>	4
1.2.1 Occurrence and Ecological Impact of Cyanobacterial Blooms in Lake Taihu.....	4
1.2.2 Effects of Temperature on the Adaptability of <i>Microcystis aeruginosa</i>	5
1.2.3 Role of Long-Chain Fatty Acids in Temperature Adaptation of <i>Microcystis aeruginosa</i>	6
1.3 Application of Multi-Omics Integration in Adaptation Mechanisms	7
1.4 Purpose of Research.....	8
2. Materials and Methods	9
2.1 Experimental Algal Strain and Cultivation	9
2.2 Experimental Instruments and reagent kits	9
2.3 Growth Rate Measurement	10
2.4 Biochemical Composition Analysis.....	10
2.4.1 Sample Collection and Preservation	10
2.4.2 ATP Quantification.....	11
2.4.3 Total Protein, Total Sugar, and Total Lipid Quantification.....	11

2.5 Multi-Omics Data Collection.....	11
2.5.1 Genomic Data Collection.....	11
2.5.2 Transcriptome Data Collection.....	11
2.5.3 Targeted Metabolomics of Long-Chain Fatty Acids	12
2.6 Validation Experiment	13
2.7 Data Analysis	14
2.7.1 Correlation Analysis Between Fatty Acids and Growth Rate	14
2.7.2 Long-Chain Fatty Acids Metabolic Flux Analysis	14
2.7.3 Fatty Acid Validation Experiment Data Analysis	14
2.7.4 Differential Gene Expression Analysis.....	15
2.7.5 Gene Ontology (GO) Enrichment Analysis.....	15
2.7.6 Weighted Gene Co-expression Network Analysis (WGCNA).....	15
3. Result.....	17
3.1 Growth Rate of <i>Microcystis aeruginosa</i>	17
3.2 Fatty Acid Content in <i>Microcystis aeruginosa</i>	18
3.3 Correlation Between Growth Rate and Total Fatty Acid Content.....	19
3.4 Long-Chain Fatty Acids Biosynthesis Pathways	20
3.5 Comparison of Long-Chain Fatty Acids Content Between Different Temperature Conditions.....	22
3.5.1 Fatty Acid Content Comparison Between Temperature Conditions	22
3.5.2 Validation Experiment Results	22
3.6 Differential Gene Expression Analysis.....	24
3.7 Gene Ontology (GO) Enrichment Analysis.....	25
3.8 Weighted Gene Co-expression Network Analysis (WGCNA).....	28

3.9 TopGO Enrichment Analysis of Key WGCNA Modules.....	29
4. Discussion.....	31
4.1 Regulation of Fatty Acid Metabolism by Temperature	31
4.2 Research Strengths, Limitations, and Future Perspectives	32
5. Conclusion	35
Appendix A.....	37
References	49

List of Tables

Table 1: Experimental Instrument	9
Table 2: Experimental Reagent Kits.....	9
Table 3: t-Test Results for the Fatty Acid Supplementation	24
Table 4: Comparison of Differentially Expressed Genes Among Groups	25

List of Figures

Figure 1: Growth Rate of <i>Microcystis aeruginosa</i> Under Different Temperature Conditions	17
Figure 2: Fatty Acid Content in <i>Microcystis aeruginosa</i> at Different Temperatures.....	18
Figure 3: Correlation Analysis Between Fatty Acids and Growth Rate.....	19
Figure 4: Long-Chain Fatty Acid Biosynthesis Pathway	21
Figure 5: Comparison of Long-Chain Fatty Acids Content Between Different Temperature Conditions	22
Figure 6: Growth Curves of <i>Microcystis aeruginosa</i> Under Fatty Acid Supplementation at 15 °C.....	23
Figure 7: GO Enrichment - Biological Processes (BP) Across 15°C, 25°C, and 29°C	25
Figure 8: GO Enrichment - Molecular Functions (MF) Across 15°C, 25°C, and 29°C.....	26
Figure 9: GO Enrichment - Cellular Components (CC) Across 15°C, 25°C, and 29°C	27
Figure 10: Weighted Gene Co-expression Network.....	29
Figure A.1: MEblue GO Enrichment - BP	37
Figure A.2: MEblue GO Enrichment - MF	38
Figure A.3: MEblue GO Enrichment - CC.....	39
Figure A.4: MEbrown GO Enrichment - BP	40
Figure A.5: MEbrown GO Enrichment - MF	41
Figure A.6: MEbrown GO Enrichment - CC	42
Figure A.7: MEpink GO Enrichment - BP	43
Figure A.8: MEpink GO Enrichment - MF	44
Figure A.9: MEpink GO Enrichment - CC.....	45
Figure A.10: METurquoise GO Enrichment - BP	46
Figure A.11: METurquoise GO Enrichment - MF	47
Figure A.12: METurquoise GO Enrichment - CC.....	48

1. Introduction

1.1 Cyanobacteria and Cyanobacterial Blooms

1.1.1 Overview of Cyanobacteria

Cyanobacteria, also known as blue-green algae, are the largest known prokaryotic organisms capable of photosynthesis and belong to the domain Bacteria.¹ They are widely distributed across diverse habitats, ranging from the poles to the equator and from marine and freshwater environments to terrestrial ecosystems.² The origin of cyanobacteria dates back approximately 3.5 billion years, making them one of the earliest life forms to perform photosynthesis.³ Through photosynthesis, cyanobacteria convert solar energy into chemical energy and release oxygen, significantly increasing the oxygen concentration in Earth's atmosphere and driving the "Great Oxidation Event."⁴⁻⁶ This transformation had a profound impact on the planet's climate and biological evolution. Many scientists believe that cyanobacteria are the ancestors of modern plants, algae, and other photosynthetic organisms. Their symbiotic relationship with eukaryotic cells is thought to have played a crucial role in the formation of eukaryotic cells, laying the foundation for the evolution of complex life.

Cyanobacteria play an essential ecological role in natural ecosystems. As primary producers in aquatic environments, they fix carbon dioxide through photosynthesis and synthesize organic matter, serving as the foundation of the aquatic food chain by providing energy and nutrients for various aquatic organisms.^{7,8} Additionally, cyanobacteria possess nitrogen-fixing capabilities. In environments lacking nitrate and ammonium, they can directly absorb atmospheric nitrogen and convert it into a form that plants can utilize, thereby playing a vital role in the global nitrogen cycle and enhancing nutrient availability in ecosystems.^{1,3} Moreover, in wetland ecosystem restoration, cyanobacteria are among the earliest settlers. They help stabilize soil and dust particles, preventing erosion, while also supplying organic matter to support the

growth of other organisms.⁹ This makes them significant contributors to ecological succession and environmental restoration.

Cyanobacteria also hold considerable value in human society. Certain species, particularly *Spirulina*, are rich in high-quality proteins, vitamins, and minerals, making them widely used in nutritional supplements and health products.^{10,11} In agriculture, cyanobacteria serve as biofertilizers and biocontrol agents, enhancing soil fertility and suppressing harmful microorganisms.¹² Furthermore, due to their ability to preferentially absorb or adsorb sodium ions, cyanobacteria show potential in improving saline-alkali soils.¹³ In environmental protection, they are applied in wastewater treatment and ecological restoration, where they contribute to pollutant absorption, degradation of harmful substances, and water quality improvement, providing crucial support for sustainable development.

1.1.2 Formation and Impacts of Cyanobacterial Blooms

When certain cyanobacteria rapidly and excessively proliferate in water bodies, they form visible surface scums or cause water discoloration, a phenomenon known as cyanobacterial blooms (or blue-green algae blooms).¹⁴ Affected waters typically appear green, blue, or brown. Cyanobacterial blooms not only degrade water quality but also disrupt ecological balance and pose serious threats to aquatic life and human health.

The occurrence and intensity of cyanobacterial blooms are influenced by multiple environmental factors, primarily involving water quality, climate conditions, and human activities.¹⁵ These factors collectively create conditions that favor cyanobacterial growth and allow them to dominate in aquatic ecosystems.

One of the main drivers of cyanobacterial blooms is eutrophication, which refers to the excessive input of nutrients, mainly nitrogen and phosphorus, into water bodies.¹⁶ These nutrients primarily come from agricultural runoff, wastewater discharge, and industrial waste. High

concentrations of nutrients promote the rapid growth of cyanobacteria, allowing them to outcompete other phytoplankton and form large-scale blooms.¹⁷

Higher temperatures also support cyanobacterial growth and reproduction. Many cyanobacterial species thrive in water temperatures above 25°C, and global warming has led to an increase in the frequency and duration of cyanobacterial blooms.¹⁸ Warmer waters also cause stratification in lakes and reservoirs, reducing vertical mixing and creating a stable environment that favors cyanobacteria.¹⁹

Slow-moving or stagnant water bodies provide an ideal environment for cyanobacterial aggregation and bloom formation.²⁰ In contrast, faster-moving or well-mixed water bodies help disrupt bloom formation and reduce its scale. Therefore, reservoirs, lakes, and ponds with restricted water exchange are more susceptible to cyanobacterial blooms.²¹

Cyanobacteria can also alter and adapt to changes in water pH. During bloom events, cyanobacteria consume carbon dioxide, raising the pH of the water, which creates an environment that is unfavorable for other phytoplankton but beneficial for cyanobacterial growth.²² Additionally, some cyanobacterial species can regulate their buoyancy, allowing them to maintain optimal light conditions at specific depths in the water.²³

Climate change impacts several factors that promote cyanobacterial blooms, including rising temperatures, altered precipitation patterns, and an increase in extreme weather events. Intense rainfall can lead to the input of nutrients into water bodies through surface runoff, while drought conditions can exacerbate water stagnation. Both situations increase the risk of cyanobacterial bloom formation

The outbreak of cyanobacterial blooms leads to a significant depletion of dissolved oxygen in the water. As cyanobacteria grow and decompose, they consume oxygen, particularly when large amounts die off.²⁴ During decomposition, bacteria further deplete oxygen,

exacerbating hypoxia. In severe cases, this can create "dead zones," where oxygen levels become too low to support aquatic life, resulting in mass fish die-offs and ecosystem collapse.

Some cyanobacteria release harmful cyanotoxins during bloom events, including neurotoxins, hepatotoxins, and dermatotoxins, which pose risks to aquatic organisms, livestock, and human health.^{25,26} These toxins are highly stable and can persist in the water even after the cyanobacterial cells die, leading to long-term contamination that affects drinking water safety and aquatic ecosystems.²⁷⁻²⁹

Excessive cyanobacterial growth also increases water turbidity, reducing light penetration and inhibiting the photosynthesis of other aquatic plants. This further decreases dissolved oxygen levels, accelerates ecosystem degradation, and shifts the aquatic community toward a less diverse and less resilient state, weakening the ecosystem's ability to recover.³⁰

Cyanobacterial blooms also diminish the aesthetic and recreational value of water bodies. Large floating mats of cyanobacteria make previously clear waters appear murky, reducing their visual appeal. Overgrowth can clog waterways, obstruct navigation, and hinder water-based recreational activities. Additionally, metabolic byproducts released by cyanobacteria can produce foul odors, such as a rotting or sewage-like smell, polluting the surrounding air and reducing the livability and recreational potential of affected areas.^{31,32}

1.2 Formation of Cyanobacterial Blooms in Lake Taihu and the Adaptation Mechanisms of *Microcystis aeruginosa*

1.2.1 Occurrence and Ecological Impact of Cyanobacterial Blooms in Lake Taihu

Lake Taihu is the third-largest freshwater lake in China and serves as a crucial water source for the Yangtze River Delta region. The lake's favorable natural conditions and abundant resources have made the Taihu Basin one of the most densely populated, highly urbanized, and economically developed regions in China. Lake Taihu not only supports diverse aquatic species and provides vital habitats for waterbirds and other wildlife but also sustains key industries such

as fisheries, tourism, and agriculture while supplying drinking water to millions of people in surrounding cities.

However, over the past few decades, nutrient enrichment caused by agricultural runoff, wastewater discharge, and industrial pollution has led to frequent cyanobacterial blooms in Lake Taihu, severely impacting the ecosystem and local economy. For example, in 2007, a massive cyanobacterial bloom triggered a drinking water crisis in Wuxi, affecting more than two million residents. Despite substantial government investments in lake restoration, the issue remains unresolved. In 2017, Lake Taihu experienced its most severe cyanobacterial bloom since 2007, with an affected area even larger than the 2007 outbreak.

Microcystis aeruginosa is the most frequently occurring and widely distributed cyanobacterium responsible for these blooms in Lake Taihu. Its growth cycle begins in May, and by July to September, it becomes the dominant species, rapidly forming large-scale blooms. The success of *M. aeruginosa* in forming extensive blooms is primarily attributed to several unique structural adaptations. First, it can produce spores to store nutrients, ensuring an energy reserve for growth.³³ Second, it regulates buoyancy using gas vesicles, allowing it to remain at an optimal depth for photosynthesis.³⁴ Additionally, its cells are surrounded by a polysaccharide-rich gelatinous sheath, which provides protection against environmental stress. Under favorable conditions, *M. aeruginosa* can form dense colonies, enhancing its competitive advantage and further stabilizing bloom formation.

1.2.2 Effects of Temperature on the Adaptability of *Microcystis aeruginosa*

Temperature plays a crucial role in regulating the growth rate, biomass accumulation, physiological metabolism, and cellular composition of *Microcystis aeruginosa*, thereby influencing its ecological competitiveness. Studies have shown that the optimal growth temperature for *M. aeruginosa* ranges from 25°C to 35°C, where its photosynthetic efficiency and growth rate reach their peak.³⁵ In contrast, temperatures above 40°C or below 15°C significantly

inhibit its growth. Furthermore, elevated temperatures promote the synthesis and release of microcystins, increasing its inhibitory effect on other phytoplankton and enhancing its ecological dominance in aquatic environments.³⁶

Temperature also indirectly regulates *M. aeruginosa* adaptability by influencing phytoplankton community structure and physicochemical conditions in water bodies. For instance, high temperatures often exacerbate water column stratification, limiting vertical nutrient exchange. However, *M. aeruginosa* can overcome this challenge by adjusting its buoyancy to remain in the well-lit surface layer, securing a more favorable ecological niche. Additionally, rising temperatures may alter cell membrane fluidity, enzyme activity, and carbon-nitrogen metabolism pathways, further enhancing its adaptability.

In recent years, global climate change and rising temperatures have become key factors contributing to cyanobacterial bloom outbreaks. Prolonged high temperatures not only extend the duration of blooms but may also increase their frequency, particularly in summer and autumn.³⁷ As climate warming continues, larger-scale and longer-lasting cyanobacterial blooms may pose a severe threat to Taihu's water quality. Therefore, studying the effects of temperature on *M. aeruginosa* adaptation mechanisms is essential for understanding bloom formation processes and providing a theoretical basis for their prediction and management.

1.2.3 Role of Long-Chain Fatty Acids in Temperature Adaptation of *Microcystis aeruginosa*

Long-chain fatty acids play a crucial role in the temperature adaptation of *M. aeruginosa*, primarily by regulating cell membrane structure, energy storage, and signal transduction.³⁸

First, temperature changes directly affect cell membrane fluidity, with fatty acid composition being a key determinant of membrane properties. In high-temperature environments, *M. aeruginosa* increases the proportion of saturated fatty acids to enhance membrane stability, preventing excessive fluidity that could lead to cellular damage.³⁹ Conversely, under low

temperatures, it increases unsaturated fatty acids to maintain membrane flexibility and permeability, ensuring normal metabolic activity.⁴⁰ This temperature-regulated mechanism allows *M. aeruginosa* to maintain physiological homeostasis under varying environmental conditions, enhancing its survival capability.

Second, fatty acids serve as energy storage molecules, providing an additional energy source when nutrient conditions fluctuate. *M. aeruginosa* can accumulate lipid reserves under favorable conditions and break them down under adverse conditions to generate ATP and carbon sources, ensuring survival and reproduction in stressful environments.⁴¹ This strategy allows *M. aeruginosa* to maintain a growth advantage in water bodies with significant temperature fluctuations.

Furthermore, certain long-chain fatty acids function as signaling molecules that regulate stress responses in *M. aeruginosa*. For example, under elevated temperatures or oxidative stress, lipid signaling pathways may activate heat shock proteins (HSPs) or other defense mechanisms, increasing stress tolerance. Additionally, fatty acid metabolism is closely linked to microcystin synthesis, as some fatty acid-derived metabolites may participate in the biosynthesis and release of microcystins, potentially influencing the toxicity level of cyanobacterial blooms.

Overall, fatty acids are not only essential structural components of *M. aeruginosa* cells but also play multiple roles in its temperature adaptation. Investigating the molecular mechanisms of fatty acid metabolism in temperature adaptation can help elucidate cyanobacterial bloom formation mechanisms and provide new intervention targets for bloom control.

1.3 Application of Multi-Omics Integration in Adaptation Mechanisms

Multi-omics data integration is a powerful approach in biological research that combines multiple layers of molecular information, including genomics, transcriptomics, proteomics, and metabolomics. Each omics layer provides unique insights into cellular processes

The integration of multi-omics data **provides** several advantages in understanding adaptive mechanisms. Instead of focusing on a single molecular layer, multi-omics reveals complex biological interactions and regulatory networks. Integrated data models help predict biological responses to environmental stressors, facilitating targeted interventions. Integrated data models help predict biological responses to environmental stressors, facilitating targeted interventions.

1.4 Purpose of Research

This study aims to investigate the adaptive mechanisms of *M. aeruginosa* under temperature variations by integrating multi-omics data, including genomics, transcriptomics, and metabolomics. The focus is on exploring the role of fatty acid metabolism in the temperature adaptation of *Microcystis aeruginosa*, providing a deeper understanding of the molecular mechanisms that enable the cyanobacterium to thrive under different temperature conditions.

By elucidating the temperature adaptation mechanisms of *M. aeruginosa*, this study provides new insights into the biological basis of cyanobacterial bloom formation. The findings contribute to a deeper understanding of the physiological and genetic responses of *M. aeruginosa* to environmental changes, support theoretical foundations for controlling and preventing cyanobacterial blooms in Lake Taihu, and offer potential applications in environmental management and mitigation strategies to address eutrophication-related water quality issues.

2. Materials and Methods

2.1 Experimental Algal Strain and Cultivation

The algal strain used in this study was *Microcystis aeruginosa* Taihu98, obtained from the Freshwater Algae Culture Collection at the Institute of Hydrobiology, Chinese Academy of Sciences. The algae were cultured in sterile BG-11 medium (1.5 mM NaNO₃, 0.04 mM K₂HPO₄, 0.075 mM MgSO₄·7H₂O, 0.025 mM CaCl₂·2H₂O, 0.006 mM citric acid, 0.03 mM ferric ammonium citrate, 0.01 mM EDTA, and trace elements, made up to 1L). The cultures were maintained under a light/dark cycle of 14 hours of light and 10 hours of darkness (L: D), with a light intensity of 100 μmol photons m⁻² s⁻¹ at 25°C. The cultures were subcultured every 7 days into fresh, sterile BG-11 medium to ensure the maintenance of exponential growth. Throughout the experimental period, all conditions, except for the temperature variations, remained constant to minimize environmental fluctuations.

2.2 Experimental Instruments and reagent kits

The instruments and reagent kits used in the experiment are listed in Table 1 and Table 2.

Table 1: Experimental Instrument

Equipment Name	Model	Manufacturer
Ultraviolet-Visible Spectrophotometer	GENESYS 140	Thermo Fisher
Low-Temperature Cold Light Source Plant Growth Chamber	DGX-6008-LED	KESHENG
Ultrasonic Cell Crusher	10221072	SCIENTZ
Laboratory Centrifuge	Sovall ST 16R	Thermo Fisher
Varioskan LUX Microplate Reader	3020-81445	Thermo Fisher
Stereo Microscope	SMZ1270	Nikon

Table 2: Experimental Reagent Kits

Product Name	Product Number	Company
ATP Assay Kit	S0026	Beyotime
Plant Soluble Sugar Content Assay Kit	AKPL008M	Boxbio
BCA Protein Assay Kit	23227	Thermo Fisher

2.3 Growth Rate Measurement

100 mL of *M. aeruginosa* cultures were grown in 250 mL Erlenmeyer flasks containing sterile BG-11 medium. Prior to the experiment, algal cultures were acclimated to the target temperatures for a minimum of five generations by transferring them from 25°C to the designated temperatures. Following acclimation, 10 mL of the temperature-adjusted cultures were transferred to fresh 250 mL flasks containing 90 mL of sterile BG-11 medium. To prevent sedimentation, the cultures were shaken 2–3 times per day. The cultures were kept under a 14-hour light and 10-hour dark photoperiod (L: D) with a light intensity of 100 $\mu\text{mol photons m}^{-2} \text{s}^{-1}$.

Samples of 2 mL were collected daily under sterile conditions and fixed in 2% Lugol's iodine solution for subsequent cell density analysis. Cell counts were performed using a hemocytometer, under an optical microscope (Olympus, Japan). Cell radius (r) was measured using a Nikon 50i optical microscope coupled with Nikon Digital Vision Software Image Analysis System. The cell volume was determined using the formula for the volume of a sphere: $V = (4/3)\pi r^3$. The specific growth rate (μ) was calculated as the slope of the natural logarithm (\ln) of cell density, measured at multiple time points during the exponential growth phase.

2.4 Biochemical Composition Analysis

2.4.1 Sample Collection and Preservation

For each macromolecule, three replicates were collected during the exponential growth phase at each temperature condition. At each temperature, 2 mL of culture was sampled to determine cell density using a hemocytometer, while 100 mL was collected for biochemical composition analysis. The samples were centrifuged at $10,000 \times g$ for 10 min at 4°C, and the supernatant was discarded. The cell pellets were then flash-frozen in liquid nitrogen and stored at -80°C for further analysis.

2.4.2 ATP Quantification

The collected pelleted cells were immediately processed and analyzed using the ATP Assay Kit.

2.4.3 Total Protein, Total Sugar, and Total Lipid Quantification

The collected cell pellet was resuspended in 2 mL of lysis buffer. Cell disruption was performed using the ultrasonic homogenizer at 300 W with a 5 s on/5 s off cycle for a total of 10 min on ice. The lysate was then centrifuged at $10,000 \times g$ for 5 min at 4°C, and the supernatant was transferred to pre-cooled 2 mL microcentrifuge tubes for biochemical analysis using the respective assay kits.

To normalize the biochemical composition data, the remaining cell pellet was resuspended, and cell density was determined using the hemocytometer. The biochemical content per unit cell volume was then calculated based on the formulas provided in the assay kits.

2.5 Multi-Omics Data Collection

2.5.1 Genomic Data Collection

The genomic data was obtained from NCBI for the *Microcystis aeruginosa* Taihu98 (NCBI BioProject ID: PRJNA81203).

2.5.2 Transcriptome Data Collection

Total RNA was extracted from the samples using the Qiagen RNeasy Micro Kit (Germantown, MD, USA) following the manufacturer's instructions. The concentration and purity of the extracted RNA were examined on a Nanodrop 2000 (Waltham, MA, USA), and RNA integrity was assessed using agarose gel electrophoresis. RNA Integrity Number (RIN) values were determined by the Agilent 2100 Bioanalyzer (Agilent Technologies, Santa Clara, CA, USA).

After rRNA removal and mRNA fragmentation, six-base random primers (random hexamers) were added to synthesize single-stranded cDNA using reverse transcriptase, with mRNA as the template. Subsequently, a second-strand synthesis reaction was performed to form a stable double-stranded cDNA structure. Library preparation was followed by sequencing on the Illumina HiSeq 2500 platform.

2.5.3 Targeted Metabolomics of Long-Chain Fatty Acids

The *M. aeruginosa* cells were collected under three different temperature conditions and transferred to small steel bead homogenization tubes. 1 mL of chloroform : methanol (v/v = 1:1) was added to each tube. The homogenization tubes were placed in a low-temperature grinding machine and ground at 50 Hz for 3 minutes, followed by sonication at low temperature for 15 minutes. The tubes were then placed at -20°C for 15 minutes. Afterward, the samples were centrifuged at 13,000 rpm for 10 minutes at 4°C, and the supernatant was transferred to an EP tube for nitrogen drying.

Next, 0.2 mL of methylation reagent was added, and the tubes were vortexed for 30 seconds and incubated in a water bath at 60°C for 30 minutes. After cooling, 0.5 mL of n-hexane was added, and the tubes were vortexed for 30 seconds and centrifuged at 13,000 rpm for 10 minutes at 4°C. The upper hexane layer was transferred to a 1.5 mL centrifuge tube and dried under nitrogen.

Subsequently, 100 µL of n-hexane was added, followed by vortexing and sonication for 10 minutes. After centrifugation at 13,000 rpm for 10 minutes at 4°C, the supernatant was carefully transferred to a sample vial for analysis.

Total RNA was extracted from the samples using the Qiagen RNeasy Micro Kit (Germantown, MD, USA) following the manufacturer's instructions.

The absolute quantification of fatty acids in the samples was conducted using an Agilent 8890B gas chromatograph coupled with an Agilent 5977B mass spectrometer (Agilent Technologies, USA), using electron impact ionization (EI) with an ionization voltage of 70 eV.

Compounds were separated on an Agilent DB-FastFAME capillary column (20 m × 0.18 mm × 0.20 μm), with helium (99.999%) used as the carrier gas at a constant flow rate of 1 mL/min. The temperature program was as follows: the initial column temperature was held at 80°C for 30 seconds, then increased to 180°C at a rate of 70°C/min, followed by an increase to 220°C at 4°C/min, and finally maintained at 240°C for 2 minutes.

A 1 μL sample was injected in split mode (50:1) with an inlet temperature of 250°C. The ion source temperature was set to 230°C, and the quadrupole temperature was set to 150°C. Data acquisition was performed in scan mode.

Identification and quantification of the compounds were carried out using MassHunter software (v10.0.707.0, Agilent Technologies, USA). The peak area of the mass spectra was plotted against the concentration of the analytes to create a linear regression standard curve for quantifying sample concentrations.

2.6 Validation Experiment

Three fatty acids—C18:3n3(9,12,15), C20:3n6(8,11,14), and C20:3n3(11,14,17)—were selected for validation based on their significant increase in content during temperature reduction (as observed in Section 2.5.3). These fatty acids were diluted to 1/100 of their intracellular content at the optimal temperature.

The experiment began by transferring the algae from the optimal temperature to the lowest temperature. Two groups were set up: the control group and the experimental group. Each group included three biological replicates. Starting from an OD680 of 0.13 (early exponential phase), 200 μL of BG11 medium was added in the control group daily. For the experimental group, 200 μL of the corresponding fatty acid solution was added daily. The fatty acid content to

be added was calculated daily based on OD values, and OD680 was measured for 10 consecutive days to monitor growth.

2.7 Data Analysis

2.7.1 Correlation Analysis Between Fatty Acids and Growth Rate

Pearson correlation test was performed using R (version 4.4.3) to assess the correlation between fatty acid content and growth rate. The Pearson correlation coefficient (cor) and its significance (P-value) were calculated. Additionally, linear regression analysis was conducted to model the relationship between the two variables, and the regression equation was derived. The results were visualized using the ggplot2 package.

2.7.2 Long-Chain Fatty Acids Metabolic Flux Analysis

Long-chain Fatty acid metabolic pathways and related genes in *M. aeruginosa* were retrieved from the KEGG database, and a fatty acid metabolic flux map was constructed. Heatmaps were generated using R to visualize the relative content changes of metabolic genes and fatty acids under three different temperatures. In the heatmaps, a redder color indicates a higher relative abundance, while a bluer color indicates a lower relative abundance. For each gene or fatty acid, the heatmap is arranged in the order of 15°C, 25°C, and 29°C. These results were integrated into the metabolic flux map to reveal how temperature variation regulates the fatty acid metabolic network.

2.7.3 Fatty Acid Validation Experiment Data Analysis

The data from the fatty acid validation experiment were statistically analyzed to evaluate the effect of exogenous fatty acid supplementation on growth. Growth curves for 10 days were plotted using R, illustrating the changes in OD680 over time for both the experimental and control groups. Independent sample t-tests were performed on the daily growth data to compare the significance of the differences (P-value) between the experimental and control groups,

evaluating the potential impact of exogenous fatty acid supplementation under low-temperature conditions.

2.7.4 Differential Gene Expression Analysis

The DESeq2 R package was used to normalize the transcriptomic data to ensure comparability across different samples. Differential gene expression (DEG) analysis was performed under different temperature conditions to identify significantly differentially expressed genes (DEGs). The normalized gene expression matrix was used to calculate the Fold Change (FC), and False Discovery Rate (FDR)-adjusted P-values were applied to ensure statistical reliability. Significant upregulated and downregulated genes were then selected for further functional enrichment analysis.

2.7.5 Gene Ontology (GO) Enrichment Analysis

Gene Ontology (GO) enrichment analysis of differentially expressed genes (DEGs) was performed using the TopGO R package to explore their enrichment in Biological Process (BP), Molecular Function (MF), and Cellular Component (CC). Fisher's exact test was used to assess the significance of enrichment, and visual methods were employed to display the significantly enriched GO terms. This analysis helped to reveal the biological processes and molecular mechanisms involved in gene expression changes under different temperature conditions.

2.7.6 Weighted Gene Co-expression Network Analysis (WGCNA)

Weighted Gene Co-expression Network Analysis (WGCNA) was used to construct a gene co-expression network and explore potential relationships between gene expression levels (TPM), fatty acid content, biomolecular characteristics, and growth curves. Clustering analysis was performed on gene expression data to identify modules highly correlated with fatty acid content. TopGO enrichment analysis was further conducted on the genes in these modules to identify their possible functional mechanisms. This analysis provided insights into the complex

relationship between fatty acid metabolism and gene expression regulation, and it helped elucidate the molecular biological basis for the impact of temperature variation on fatty acid metabolism in *Microcystis aeruginosa*.

3. Result

3.1 Growth Rate of *Microcystis aeruginosa*

In this study, we measured the growth rate of *Microcystis aeruginosa* Taihu 98 under eight temperature conditions: 13, 15, 17, 20, 23, 25, 29, and 33°C (Figure 1). The results showed that at 13°C, the growth of *M. aeruginosa* was severely inhibited, with a decreasing cell density (negative growth rate), indicating that this temperature was unfavorable for its survival. As the temperature increased to 15°C and above, the growth rate gradually increased, with a significant surge observed between 23°C and 25°C. Starting from 25°C, the growth rate increase slowed, reaching its peak at 29°C. However, as the temperature further increased to 33°C, the growth rate began to decline.

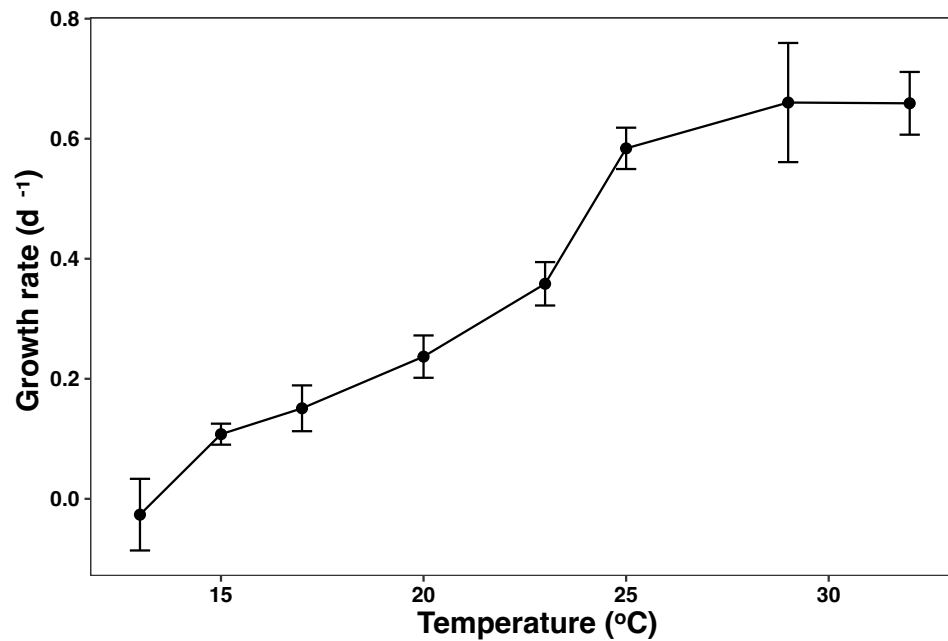


Figure 1: Growth Rate of *Microcystis aeruginosa* Under Different Temperature Conditions

Overall, *M. aeruginosa* exhibited high growth activity between 25°C and 29°C, with the maximum growth rate observed at 29°C. This trend aligns with the natural bloom cycle of *M. aeruginosa* in Lake Taihu. Based on these findings, we selected 15°C as the lower temperature

limit for *M. aeruginosa* growth, 25°C as the representative temperature for its rapid growth phase, and 29°C as the optimal growth temperature for further studies.

3.2 Fatty Acid Content in *Microcystis aeruginosa*

The total fatty acid, saturated fatty acid (SFA), and unsaturated fatty acid (UFA) contents of *Microcystis aeruginosa* were measured at three different temperatures (Figure 2). The results showed that at 25°C, the total fatty acid content was significantly higher than at the other two temperatures. Similarly, both SFA and UFA contents were also highest at 25°C.

Additionally, at all three temperatures, the UFA content was consistently higher than the SFA content, indicating a dominant presence of unsaturated fatty acids in *Microcystis aeruginosa* across different thermal conditions. This suggests that temperature plays a crucial role in regulating fatty acid synthesis, with 25°C being the most favorable condition for fatty acid accumulation.

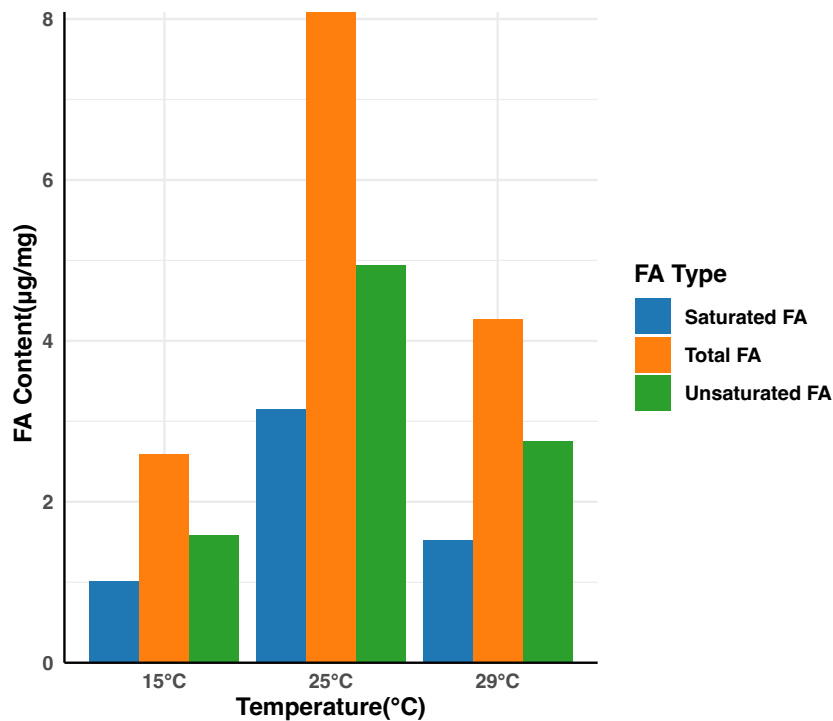


Figure 2: Fatty Acid Content in *Microcystis aeruginosa* at Different Temperatures

3.3 Correlation Between Growth Rate and Total Fatty Acid Content

To examine the relationship between growth rate and total fatty acid content, a Pearson correlation analysis was performed. The results showed a strong positive correlation between the two variables, with a Pearson correlation coefficient of 0.83 and a statistically significant P-value of 0.0056 (Figure 3).

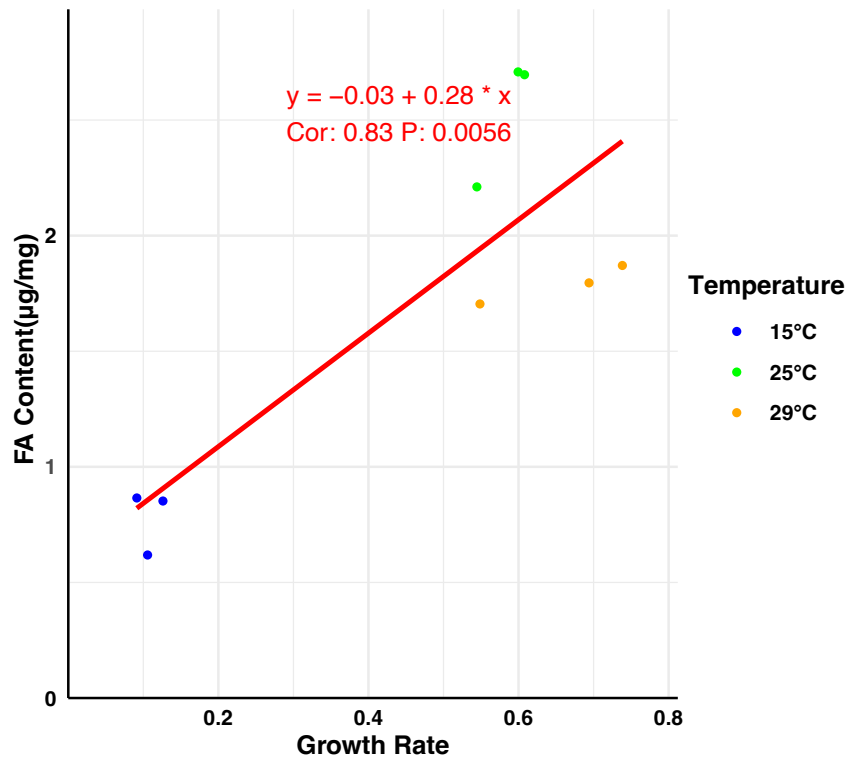


Figure 3: Correlation Analysis Between Fatty Acids and Growth Rate

Furthermore, linear regression analysis revealed a positive linear relationship, described by the equation:

$$y = -0.03 + 0.28x$$

y represents the total fatty acid content and x represents the growth rate. The fitted regression line indicates that higher growth rates are associated with enhanced fatty acid accumulation in *Microcystis aeruginosa*, highlighting a potential link between cell proliferation and lipid metabolism under different temperature conditions.

3.4 Long-Chain Fatty Acids Biosynthesis Pathways

According to the gene heatmap results (Figure 4), the relative expression levels of genes encoding enzymes involved in the synthesis of long-chain fatty acids from C12:0 to C18:1(9) were the lowest at 25°C. In the subsequent synthesis process, the expression levels of genes related to the conversion from C18:1(9) to C18:2(9,12) decreased as the temperature increased, suggesting a potential reduction in the production of C18:2(9,12). However, in the conversion from C18:2(9,12) to C18:3(6,9,12), gene expression levels increased with rising temperatures, indicating that higher temperatures promoted the synthesis of C18:3(6,9,12). Additionally, during the conversion from C18:2(9,12) to C18:3(9,12,15), gene expression was highest at 25°C, suggesting that this temperature was most favorable for the synthesis of C18:3(9,12,15).

From the heatmap of long-chain fatty acid content, most fatty acids showed the highest relative abundance at 25°C and the lowest at 15°C, except for C18:3(9,12,15), C20:3(8,11,14), and C20:3(11,14,17), which had the lowest content at 29°C. Combining gene expression changes and fatty acid content variations, in most cases, when the temperature was either increased or decreased from 25°C, the expression of fatty acid biosynthesis-related genes increased, whereas the fatty acid content decreased. This suggests that under these conditions, the consumption rate of fatty acids may have exceeded their synthesis rate, leading to a net reduction in fatty acid accumulation.

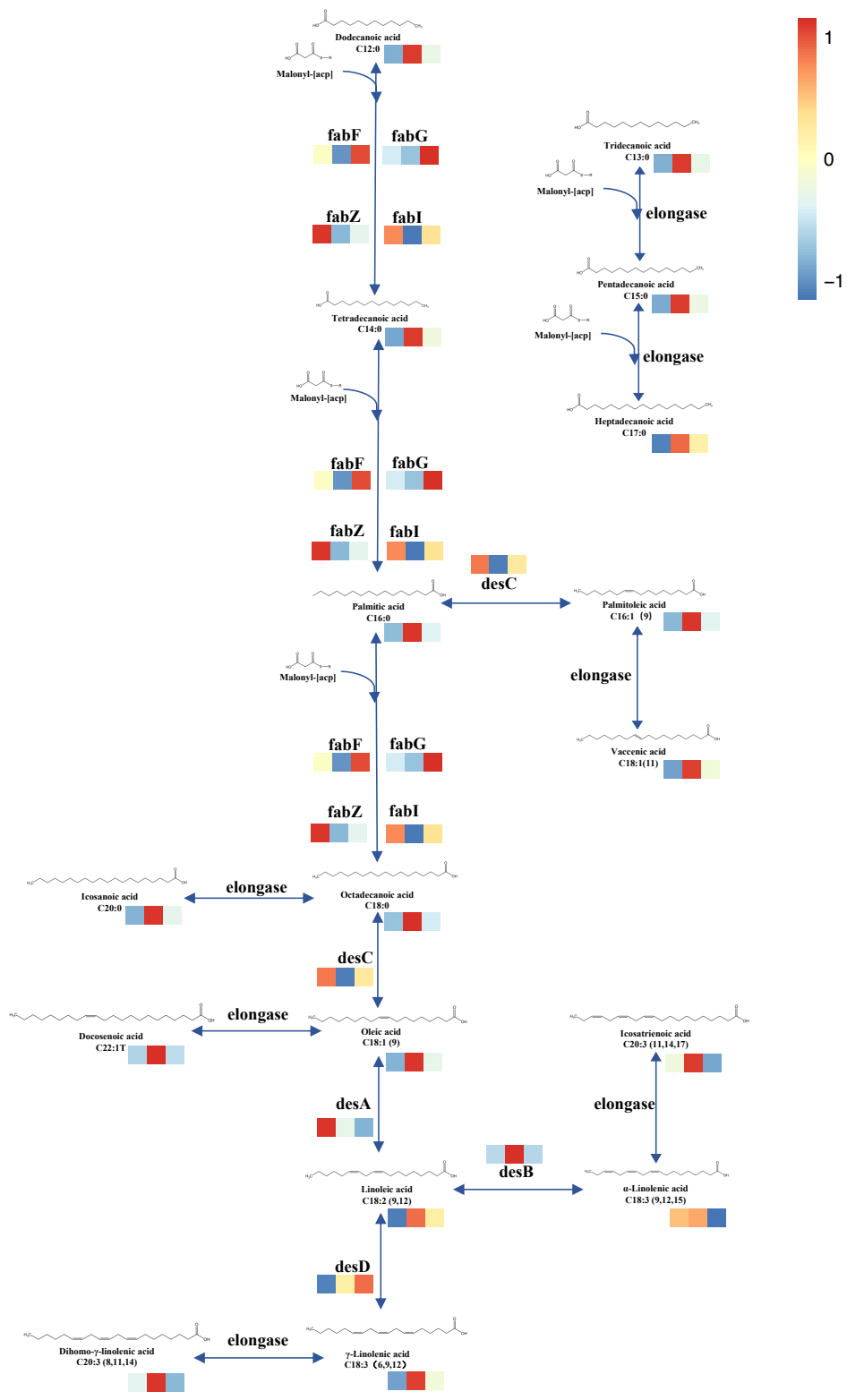


Figure 4: Long-Chain Fatty Acid Biosynthesis Pathway

3.5 Comparison of Long-Chain Fatty Acids Content Between Different Temperature Conditions

3.5.1 Fatty Acid Content Comparison Between Temperature Conditions

To determine which fatty acids should be included in the validation experiment, we compared the content of long-chain fatty acids between 29°C and 15°C. The results showed that, compared to 29°C, only C18:3n3(9,12,15), C20:3n6(8,11,14), and C20:3n3(11,14,17) exhibited an increase in content at 15°C (Figure 5). Based on this observation, these three fatty acids were selected for further validation in the fatty acid supplementation experiment.

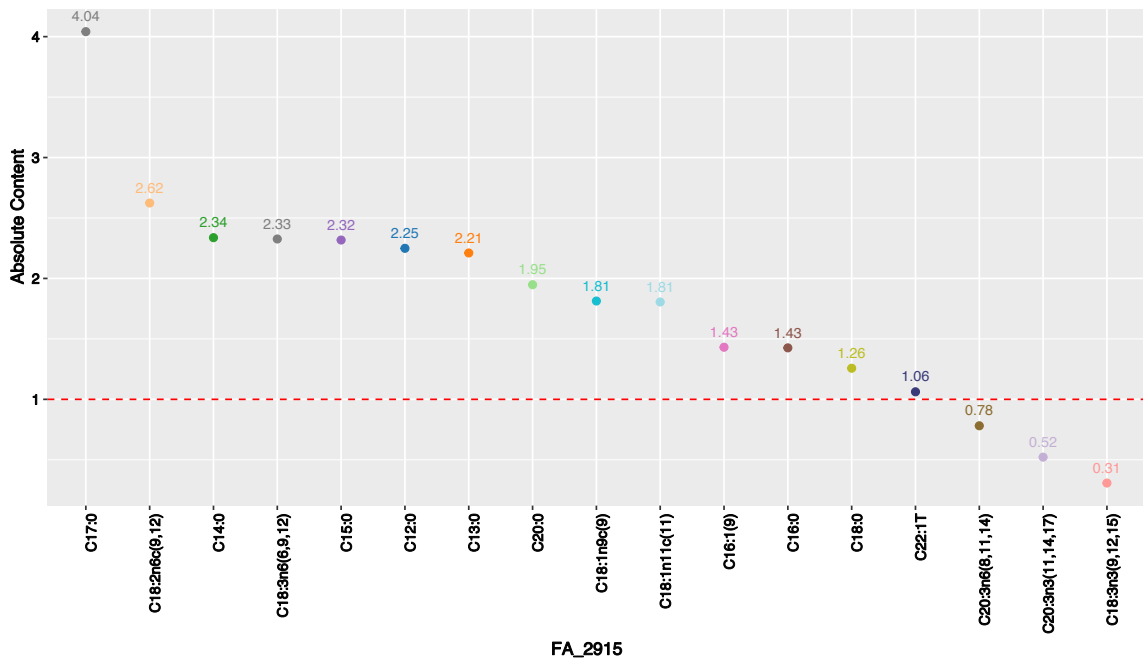


Figure 5: Comparison of Long-Chain Fatty Acids Content Between Different Temperature Conditions

3.5.2 Validation Experiment Results

The results of the validation experiment (Figure 5) showed that, starting from the second day after fatty acid supplementation, the experimental groups exhibited improved growth compared to the control group, as indicated by higher OD680 values.

Statistical analysis using independent sample t-tests further confirmed these observations. From the third day onward, the group supplemented with C18:3n3(9,12,15) showed a significant

increase in growth compared to the control group. Meanwhile, the groups supplemented with C20:3n6(8,11,14) and C20:3n3(11,14,17) exhibited significant growth enhancement from the seventh day onward (Table 3). These findings suggest that exogenous supplementation with these fatty acids can promote the growth of *M.aeruginosa* under low-temperature conditions, with C18:3n3(9,12,15) having a more immediate effect.

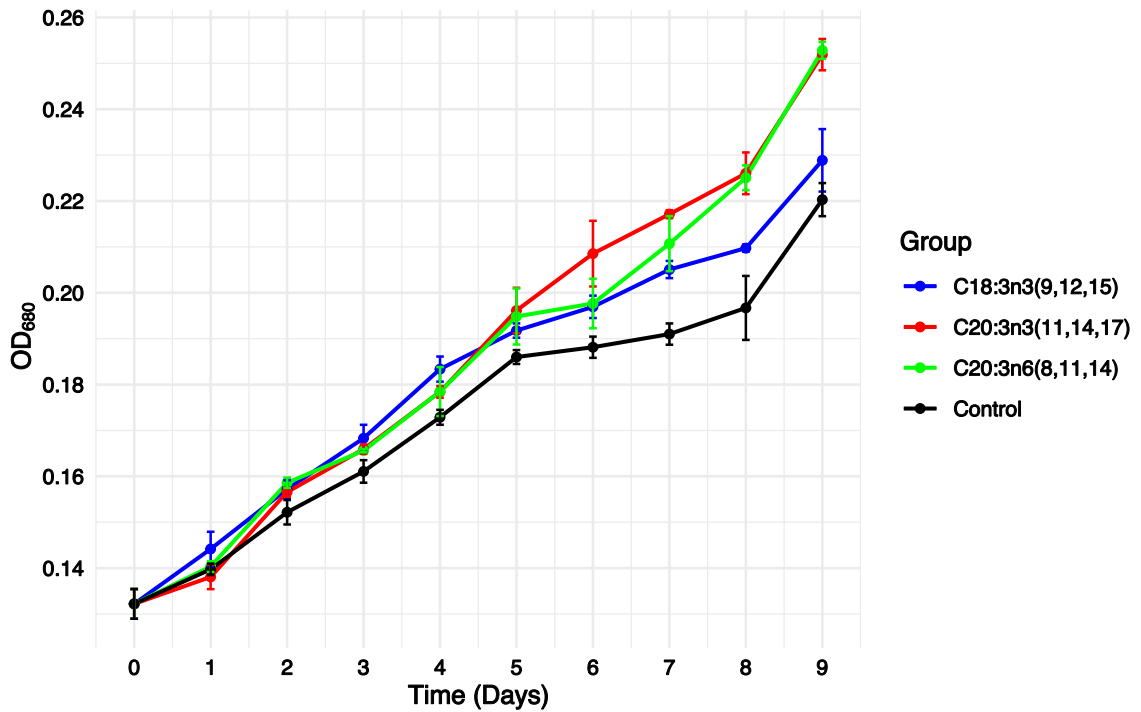


Figure 6: Growth Curves of *Microcystis aeruginosa* Under Fatty Acid Supplementation at 15 °C

Table 3: t-Test Results for the Fatty Acid Supplementation

Date	Group Comparison	P value
0	C18:3n3(9,12,15) vs control	1
1	C18:3n3(9,12,15) vs control	0.168323
2	C18:3n3(9,12,15) vs control	0.063157
3	C18:3n3(9,12,15) vs control	0.032014
4	C18:3n3(9,12,15) vs control	0.008515
5	C18:3n3(9,12,15) vs control	0.010083
6	C18:3n3(9,12,15) vs control	0.010674
7	C18:3n3(9,12,15) vs control	0.001463
8	C18:3n3(9,12,15) vs control	0.081721
9	C18:3n3(9,12,15) vs control	0.148457
0	C20:3n6(8,11,14) vs control	1
1	C20:3n6(8,11,14) vs control	0.577088
2	C20:3n6(8,11,14) vs control	0.037297
3	C20:3n6(8,11,14) vs control	0.082844
4	C20:3n6(8,11,14) vs control	0.204927
5	C20:3n6(8,11,14) vs control	0.121868
6	C20:3n6(8,11,14) vs control	0.075676
7	C20:3n6(8,11,14) vs control	0.01889
8	C20:3n6(8,11,14) vs control	0.011123
9	C20:3n6(8,11,14) vs control	0.000818
0	C20:3n3(11,14,17) vs control	1
1	C20:3n3(11,14,17) vs control	0.400675
2	C20:3n3(11,14,17) vs control	0.089103
3	C20:3n3(11,14,17) vs control	0.05932
4	C20:3n3(11,14,17) vs control	0.011141
5	C20:3n3(11,14,17) vs control	0.060742
6	C20:3n3(11,14,17) vs control	0.02914
7	C20:3n3(11,14,17) vs control	0.000888
8	C20:3n3(11,14,17) vs control	0.005865
9	C20:3n3(11,14,17) vs control	0.000391

3.6 Differential Gene Expression Analysis

We performed differential gene expression (DGE) analysis using DESeq2 to compare gene expression changes under different temperature conditions. The results showed that temperature variations had a significant impact on gene expression. The number of differentially expressed genes (DEGs) was higher in the 15°C vs 25°C and 15°C vs 29°C groups, with 1,770 and 1,782 DEGs, respectively, while the 29°C vs 25°C group had relatively fewer DEGs (1,384) (Table 4). Overall, low temperature (15°C) had a greater impact on gene expression compared to

moderate (25°C) and high (29°C) temperatures, leading to more significant gene expression changes. This suggests that organisms may require broader gene regulation to adapt to environmental stress under low-temperature conditions.

Table 4: Comparison of Differentially Expressed Genes Among Groups

Comparison (Experiment vs Control)	Upregulated Genes	Downregulated Genes	Total DEGs
15 °C vs 25 °C	870	900	1770
29 °C vs 25 °C	759	625	1384
15 °C vs 29 °C	848	934	1782

3.7 Gene Ontology (GO) Enrichment Analysis

In this study, we explored the impact of temperature variation on different biological processes, molecular functions, and cellular components through Gene Ontology (GO) enrichment analysis. Temperature changes resulted in significant gene expression variations across multiple domains, and we present a detailed summary of these results below.

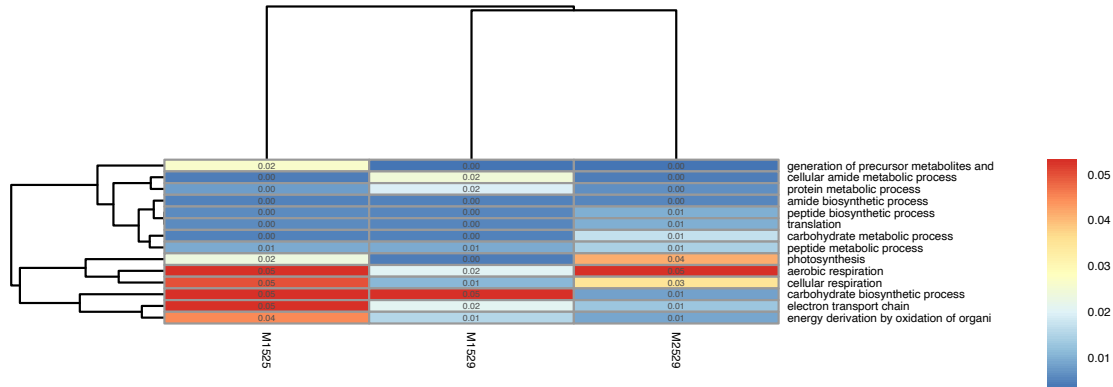


Figure 7: GO Enrichment - Biological Processes (BP) Across 15°C, 25°C, and 29°C

Temperature variation significantly affected several biological processes related to metabolism and energy conversion. Specifically, key processes such as protein metabolism, amide synthesis, peptide synthesis, and energy metabolism processes like aerobic respiration, cellular respiration, and the electron transport chain all showed significant changes. These changes suggest that temperature regulates important metabolic pathways within the cell,

potentially linked to cellular energy balance and biosynthetic activities. Additionally, processes related to photosynthesis, such as photosynthesis and photosystem II, also exhibited significant changes with temperature variation. The enrichment of these processes indicates that temperature changes have a major impact on the photosynthetic and energy conversion functions of plants or microorganisms, further emphasizing the role of temperature in cellular energy acquisition and metabolic regulation.

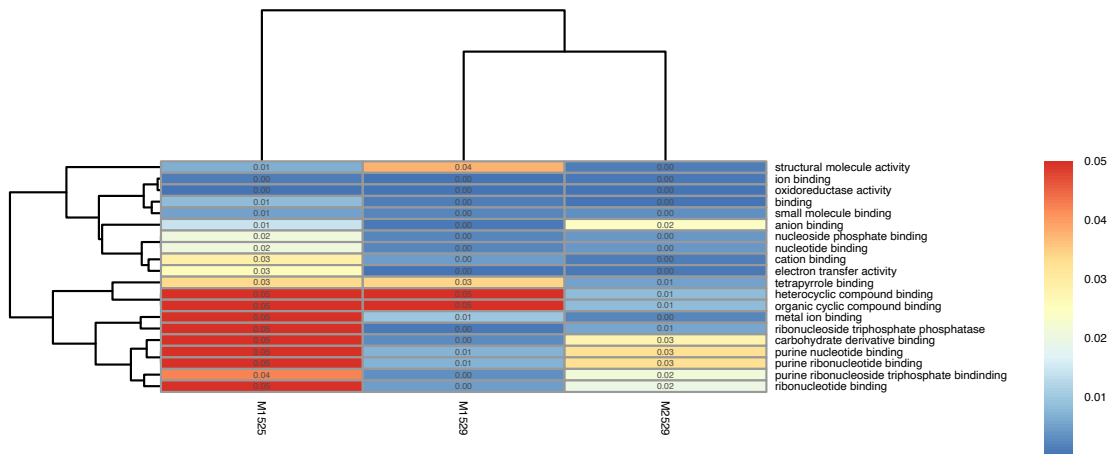


Figure 8: GO Enrichment - Molecular Functions (MF) Across 15°C, 25°C, and 29°C

The impact of temperature variation on molecular functions primarily manifests in two areas: First, temperature changes significantly influenced molecular interactions and binding abilities within the cell, particularly functions related to ion binding, nucleotide phosphate binding, and purine nucleotide binding. These changes could regulate the interaction strength between different molecules within the cell, thereby affecting the overall biological activity of the cell. Second, the enrichment of functions related to energy conversion, such as oxidoreductase activity and electron transfer activity, suggests that temperature variation plays a key role in regulating cellular metabolism, especially in electron transfer, redox reactions, and energy generation processes.

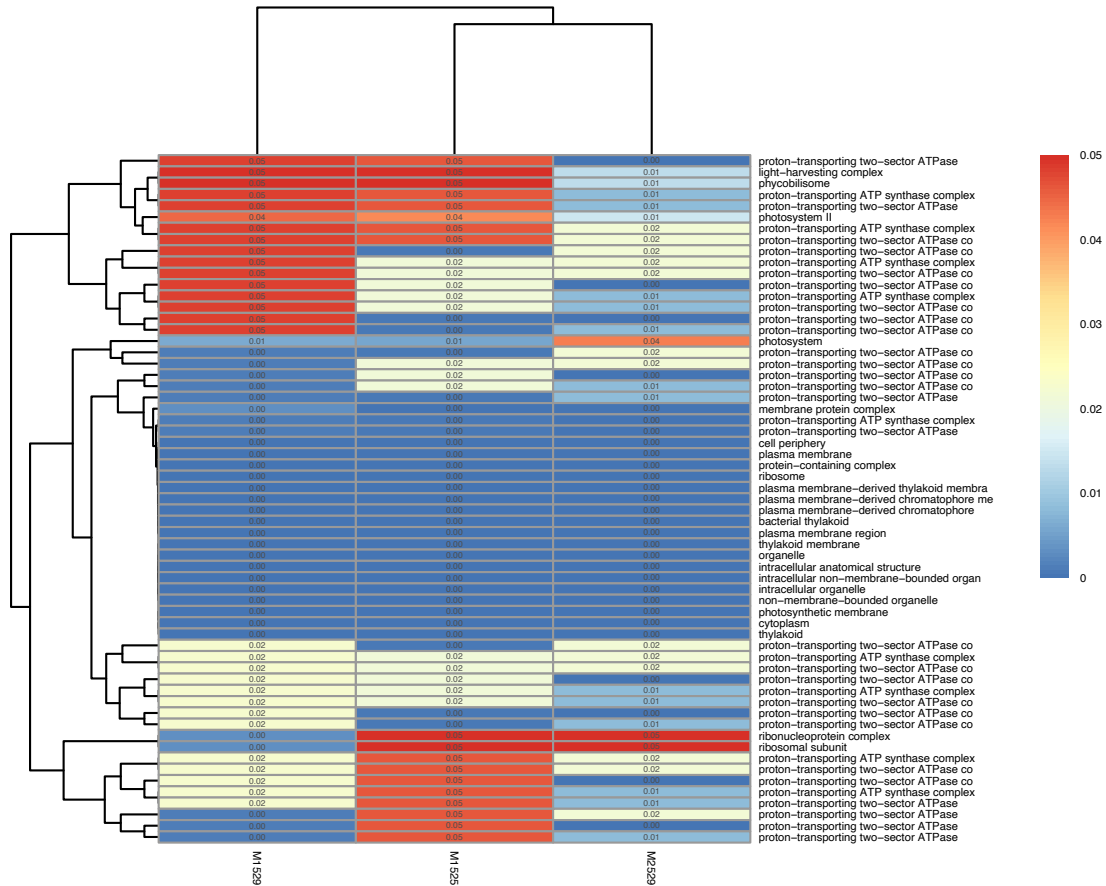


Figure 9: GO Enrichment - Cellular Components (CC) Across 15°C, 25°C, and 29°C

Temperature variation also had a significant impact on cellular components associated with energy conversion and cellular structure, specifically in two areas: First, components related to energy conversion, such as the proton transport ATP synthase complex, photosystem II, and the plasma membrane, are involved in cellular energy synthesis and conversion, indicating that temperature changes might regulate key structures involved in cellular energy acquisition. Second, in terms of cellular structure and function regulation, the enrichment of membrane protein complexes, ribosomes, and ribonucleoprotein complexes suggests that temperature variation affects the composition of cellular structures, particularly organelles involved in protein synthesis and cellular function execution. These results indicate that temperature changes not

only regulate the biological functions of the cell but also help the cell adapt to environmental changes by altering its structure and functions.

In conclusion, temperature variation significantly affects multiple metabolic processes, molecular functions, and cellular components, regulating key biological processes such as cellular energy metabolism, protein synthesis, and molecular interactions within the cell.

3.8 Weighted Gene Co-expression Network Analysis (WGCNA)

To investigate the potential regulatory relationships between gene expression and fatty acid metabolism under different temperature conditions, we performed Weighted Gene Co-expression Network Analysis (WGCNA). This analysis identified several gene modules that exhibited significant correlations with fatty acid content, temperature, and other biomolecular characteristics (Figure 10).

Among these modules, the MEBrown module displayed a strong negative correlation with all long-chain fatty acids except for C18:2n6c and C18:3n3, suggesting a potential role in fatty acid biosynthesis or degradation pathways.

The MEPink module showed a significant positive correlation with C18:3n6 ($r = 0.74$, $p = 0.02$), whereas the MEBlue module exhibited an even stronger positive correlation with C18:3n3 ($r = 0.90$, $p = 0.0008$). These findings suggest that genes within these modules may be involved in the regulation of polyunsaturated fatty acid metabolism.

Notably, the METurquoise module stood out as the only module significantly correlated with temperature ($r = -1$, $p = 3e-9$). Additionally, genes in this module showed a strong negative correlation with C17:0, growth rate, total protein, and total sugar, while displaying a positive correlation with ATP and total fatty acid content. This suggests that the METurquoise module plays a crucial role in temperature-mediated metabolic regulation, potentially affecting both energy production and lipid metabolism.

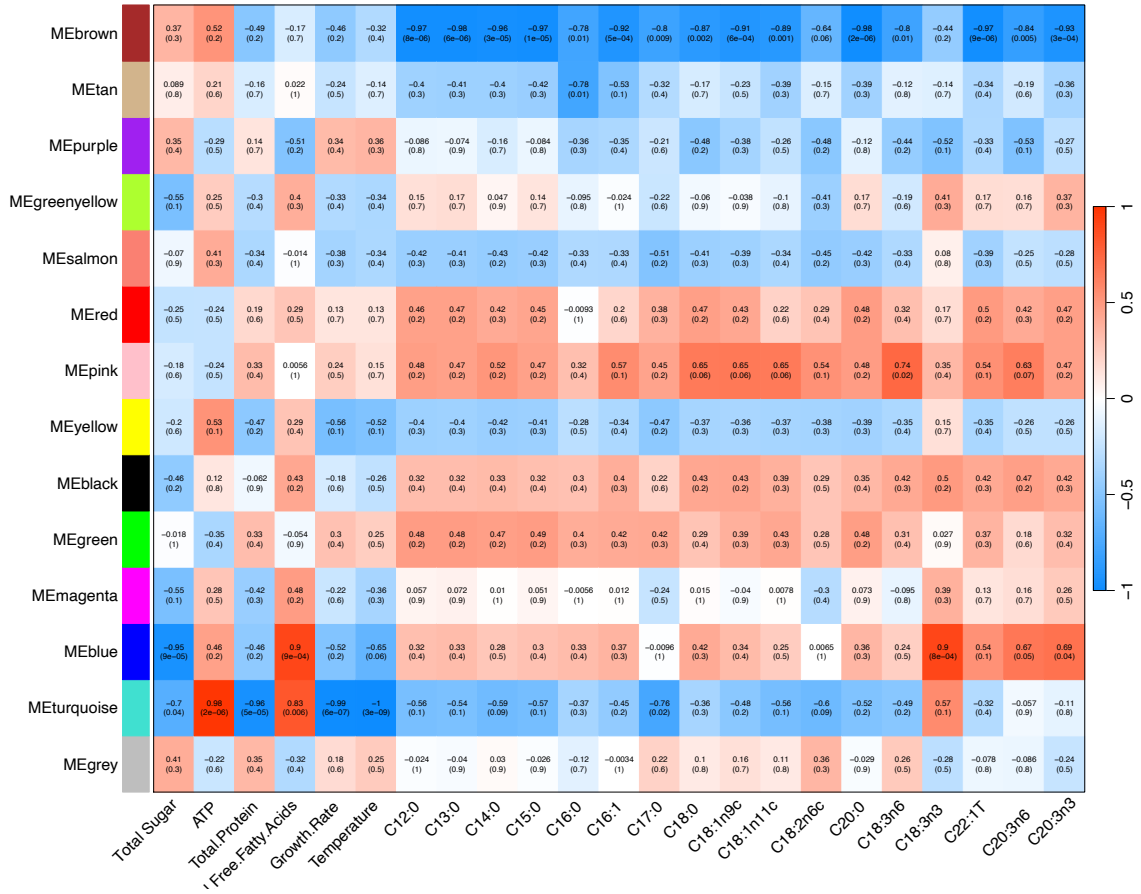


Figure 10: Weighted Gene Co-expression Network

3.9 TopGO Enrichment Analysis of Key WGCNA Modules

The MEblue module genes are primarily enriched in carbon metabolism and lipid metabolism, involving mitochondrial functions and ion transport. The enriched cellular components are mainly located in the mitochondrial membrane and respiratory chain complexes, suggesting that this module may regulate mitochondrial energy metabolism and the electron transport chain, thereby influencing fatty acid synthesis and degradation (Figure A.1-3).

The MEbrown module genes are mainly involved in fundamental metabolism and protein synthesis, enriched in ribosomes and ATP synthesis-related structures, with catalytic activity. This suggests that the module may play a crucial role in energy metabolism and fatty acid

degradation by promoting specific enzymatic activities to meet cellular metabolic demands (Figure A.4-6).

The MEpink module genes are associated with photosynthesis and transmembrane transport, primarily enriched in the photosynthetic electron transport chain and various transport functions. These genes are located in the chloroplast, cell membrane, and transmembrane complexes, indicating that this module may influence fatty acid precursor synthesis and energy metabolism by regulating light energy conversion and metabolite transport (Figure A.5-9).

The METurquoise module genes appear to be temperature-regulated, mainly enriched in DNA replication, metal ion binding, and cytoskeletal functions. The associated cellular components are involved in maintaining cellular structural stability and membrane complexes, suggesting that this module may regulate cell proliferation, metabolic control, and environmental adaptation, indirectly impacting energy and lipid metabolism (Figure A.10-12).

4. Discussion

4.1 Regulation of Fatty Acid Metabolism by Temperature

The impact of temperature on the ratio of unsaturated and saturated fatty acids has been widely observed across various organisms, including bacteria, animals, and plants.^{42,43} This phenomenon is generally explained as an adaptive strategy by which organisms dynamically adjust their fatty acid composition to maintain membrane fluidity and function under different temperature conditions. Our study confirms this pattern in *Microcystis aeruginosa*, showing that the content of long-chain fatty acids (MLCFAs) varies significantly with temperature. Specifically, we found that under extreme temperatures (both high and low), many genes involved in fatty acid biosynthesis were significantly upregulated, while MLCFA consumption increased. This suggests that temperature stress not only influences fatty acid synthesis but also promotes its degradation to optimize membrane fluidity and permeability, thereby maintaining normal physiological functions.⁴⁴

Furthermore, we validated the critical role of MLCFAs in temperature adaptation through exogenous supplementation experiments. The addition of significantly increased MLCFAs, such as C18:3n3(9,12,15), C20:3n6(8,11,14), and C20:3n3(11,14,17), significantly improved *M. aeruginosa* growth under low-temperature conditions. This finding aligns with previous studies, which suggest that a higher proportion of polyunsaturated fatty acids (PUFAs) enhances membrane flexibility, allowing organisms to better tolerate cold environments.^{45,46} In contrast, under high-temperature conditions, cells may increase the proportion of saturated fatty acids to enhance membrane stability and prevent excessive fluidization, consistent with known temperature adaptation mechanisms.⁴⁷

To further elucidate the regulatory mechanisms of fatty acid metabolism under temperature stress, we employed weighted gene co-expression network analysis (WGCNA) to identify key gene modules closely associated with fatty acid metabolism and temperature

adaptation. Functional enrichment analysis (TopGO) revealed that these gene modules were primarily involved in carbon metabolism and lipid metabolism, particularly in mitochondrial function and ion transport. For instance, genes in the MEblue module were significantly enriched in carbon and lipid metabolism pathways, including mitochondrial membrane and respiratory chain complexes, suggesting that this module plays a central role in regulating fatty acid synthesis and degradation. Since mitochondria are key organelles for energy metabolism, their functional changes could influence fatty acid production and breakdown, ultimately affecting membrane fluidity and permeability, enabling *M. aeruginosa* to respond more effectively to temperature fluctuations.

Notably, changes in fatty acid composition not only influence the physical properties of membranes but may also trigger a cascade of metabolic responses. For example, temperature shifts may regulate the expression of fatty acid metabolism-related genes, thereby impacting energy metabolism, redox balance, and signal transduction pathways. These metabolic adjustments help optimize cellular energy and resource utilization, enhancing tolerance to temperature variations. Additionally, previous studies have indicated that temperature changes may further regulate fatty acid metabolism genes through transcription factors and epigenetic modifications, such as DNA methylation and histone modifications. Thus, our study not only sheds light on the mechanisms underlying *M. aeruginosa*'s response to temperature fluctuations but also provides new perspectives for exploring its potential regulatory networks.

4.2 Research Strengths, Limitations, and Future Perspectives

This study employed an integrative multi-omics approach, including genomics, transcriptomics, and metabolomics, to systematically analyze the temperature adaptation mechanisms of *Microcystis aeruginosa* at multiple levels. This comprehensive strategy not only offers a more holistic perspective but also further supports the role of temperature as a key environmental factor regulating fatty acid metabolism. Moreover, it highlights the importance of

MLCFAs in the temperature adaptation of *Microcystis aeruginosa*. These findings not only deepen our understanding of cyanobacterial adaptation strategies but also provide a theoretical basis for optimizing industrial microalgae cultivation conditions and improving biofuel production efficiency.

Despite utilizing a multi-omics approach to analyze the effects of temperature on fatty acid metabolism in *Microcystis aeruginosa* and uncovering the critical role of MLCFAs in temperature adaptation, some limitations remain, requiring further investigation. First, this study did not examine the response of *Microcystis aeruginosa* to extremely high temperatures (>29°C). Extreme heat may trigger distinct metabolic regulatory mechanisms, and studying the physiological and molecular adaptation processes under such conditions could help elucidate the thermal tolerance limits and survival strategies of *Microcystis aeruginosa*. Second, our study primarily focused on metabolic and transcriptional responses to short-term temperature fluctuations, while microbial temperature adaptation is often a long-term dynamic process involving gene expression remodeling and metabolic homeostasis regulation. Future research should incorporate long-term cultivation experiments to analyze the dynamic changes in gene regulation and metabolic pathways during temperature adaptation, allowing for the identification of key drivers of long-term adaptation.

Furthermore, although this study integrated genomic, transcriptomic, and metabolomic data, it did not incorporate proteomics and metabolic flux analysis. Protein-level regulation and metabolic flux changes are essential for understanding metabolic reprogramming under temperature stress. Future studies should incorporate multi-omics integration, including proteomics and fluxomics, to construct a more comprehensive regulatory network and elucidate how temperature influences lipid metabolism, cellular homeostasis, and growth regulation. Lastly, while *Microcystis aeruginosa* is a dominant species in cyanobacterial blooms, different cyanobacteria may adopt diverse temperature adaptation strategies, such as relying on antioxidant

systems or modifying membrane lipids to optimize survival. This study did not include cross-species comparisons, limiting our understanding of the overall adaptation mechanisms of cyanobacterial blooms. Future research should incorporate multiple cyanobacterial species to explore the commonalities and specificities of temperature adaptation, providing a more theoretically grounded approach for the ecological regulation of cyanobacterial blooms.

In summary, this study lays the foundation for understanding the temperature adaptation mechanisms of *Microcystis aeruginosa* and identifies the critical role of MLCFAs in this process. However, to fully uncover the complexity of temperature regulation on cyanobacterial metabolism, further systematic studies are needed. Expanding experimental conditions, integrating multi-omics analyses, conducting long-term adaptation studies, and performing cross-species comparisons will enhance our understanding of cyanobacterial ecological adaptation and provide scientific insights for predicting and managing cyanobacterial blooms.

5. Conclusion

This study presents a comprehensive multi-omics approach to investigate the temperature adaptation mechanisms of *Microcystis aeruginosa*, shedding light on the intricate relationship between temperature stress and fatty acid metabolism. By integrating genomics, transcriptomics, and metabolomics data, we identified key temperature-regulated pathways, emphasizing the critical role of long-chain fatty acids (MLCFAs) in maintaining membrane fluidity and cellular function under varying thermal conditions.

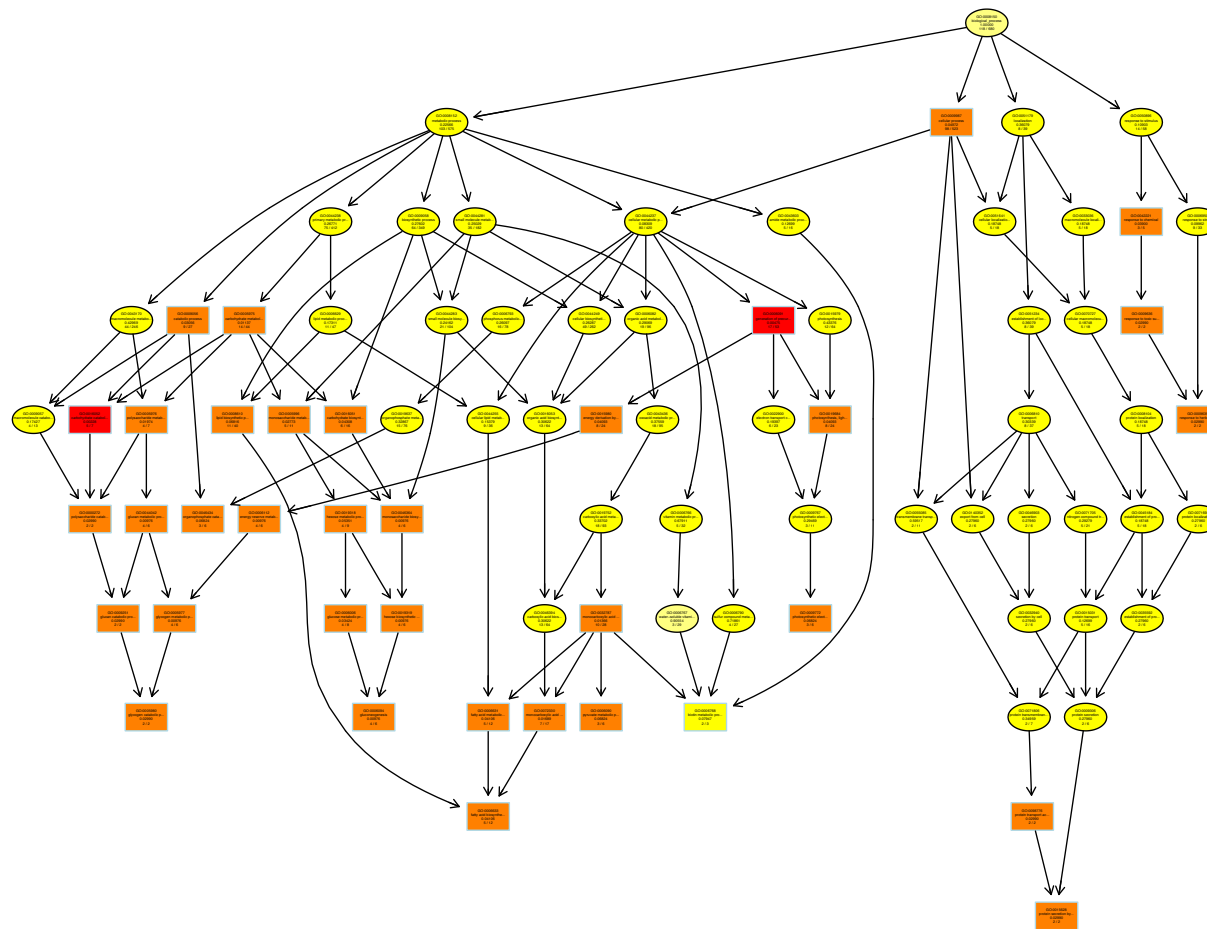
Our findings highlight that *M. aeruginosa* dynamically adjusts its fatty acid composition in response to temperature fluctuations, with upregulation of fatty acid biosynthesis and increased MLCFA consumption under extreme temperatures. Exogenous supplementation experiments further validated the essential role of polyunsaturated fatty acids in enhancing cold tolerance and the increased saturation of fatty acids contributing to heat tolerance. These results provide a deeper understanding of the molecular mechanisms underlying temperature adaptation in cyanobacteria, which is crucial for improving industrial applications like microalgae cultivation and biofuel production.

Despite these advancements, our study also points to several limitations, including the lack of examination of extreme high-temperature responses and the need for long-term studies to investigate the dynamics of gene expression and metabolic pathways over time. Future research should address these gaps by incorporating proteomics, metabolic flux analysis, and cross-species comparisons to offer a more complete picture of cyanobacterial adaptation strategies to temperature stress.

Overall, this study lays a solid foundation for understanding the temperature regulation of fatty acid metabolism in *M. aeruginosa* and offers valuable insights into the ecological and industrial implications of cyanobacterial blooms. Further exploration of these mechanisms will

contribute to better management strategies for cyanobacterial blooms and optimization of algal-based biofuel production.

Appendix A: TopGO Enrichment Analysis of Key WGCNA Modules



37

Figure A.1: MEblue GO Enrichment - BP

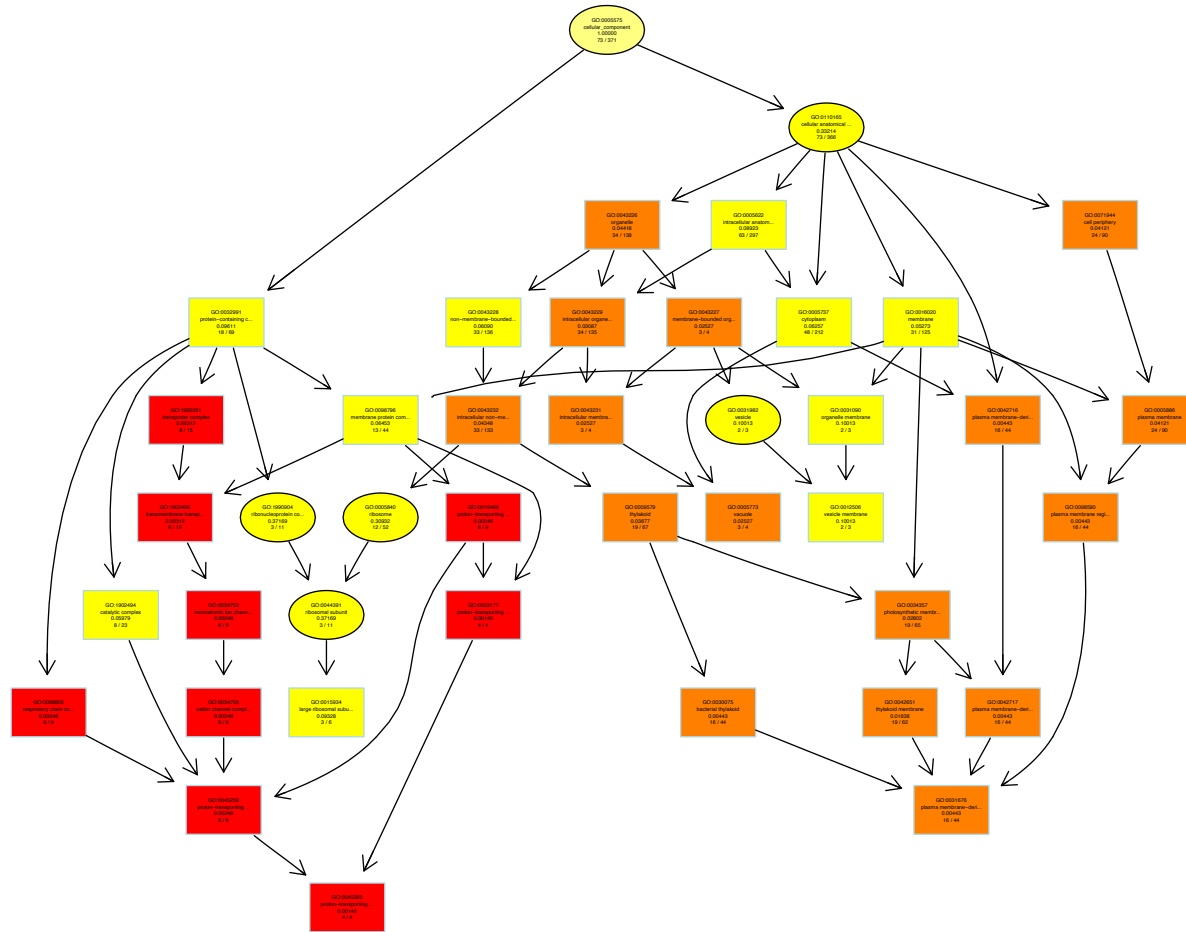


Figure A.3: MEblue GO Enrichment - CC

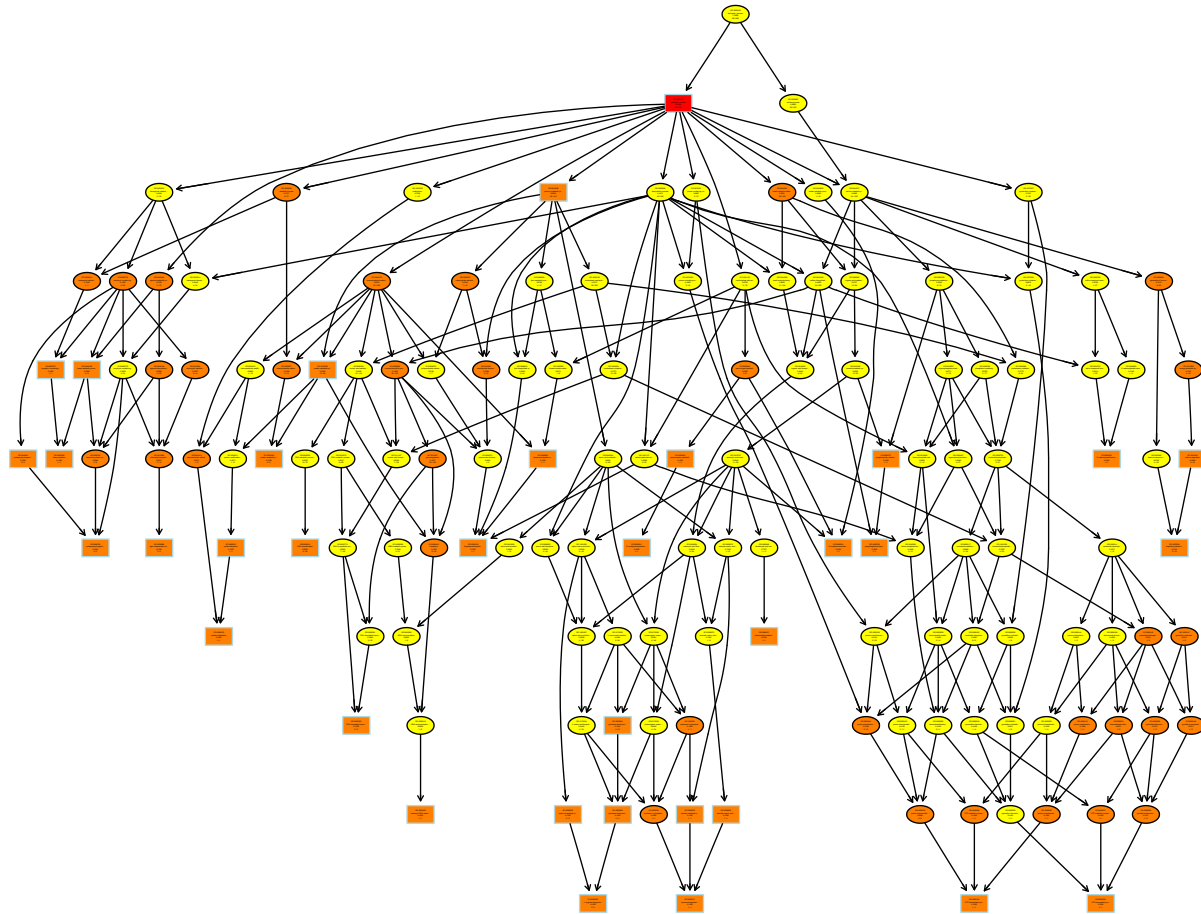


Figure A.4: MEbrown GO Enrichment - BP

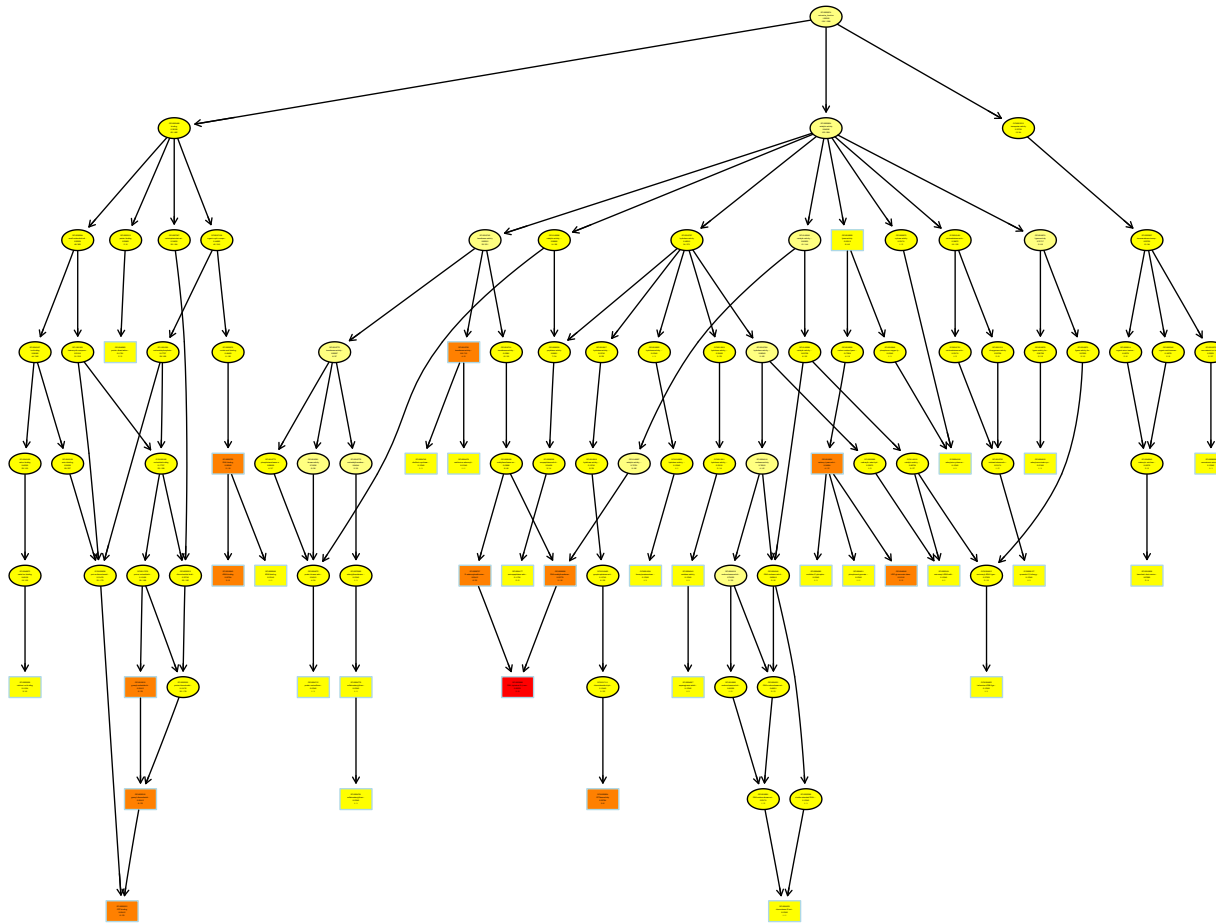


Figure A.6: MEbrown GO Enrichment - CC

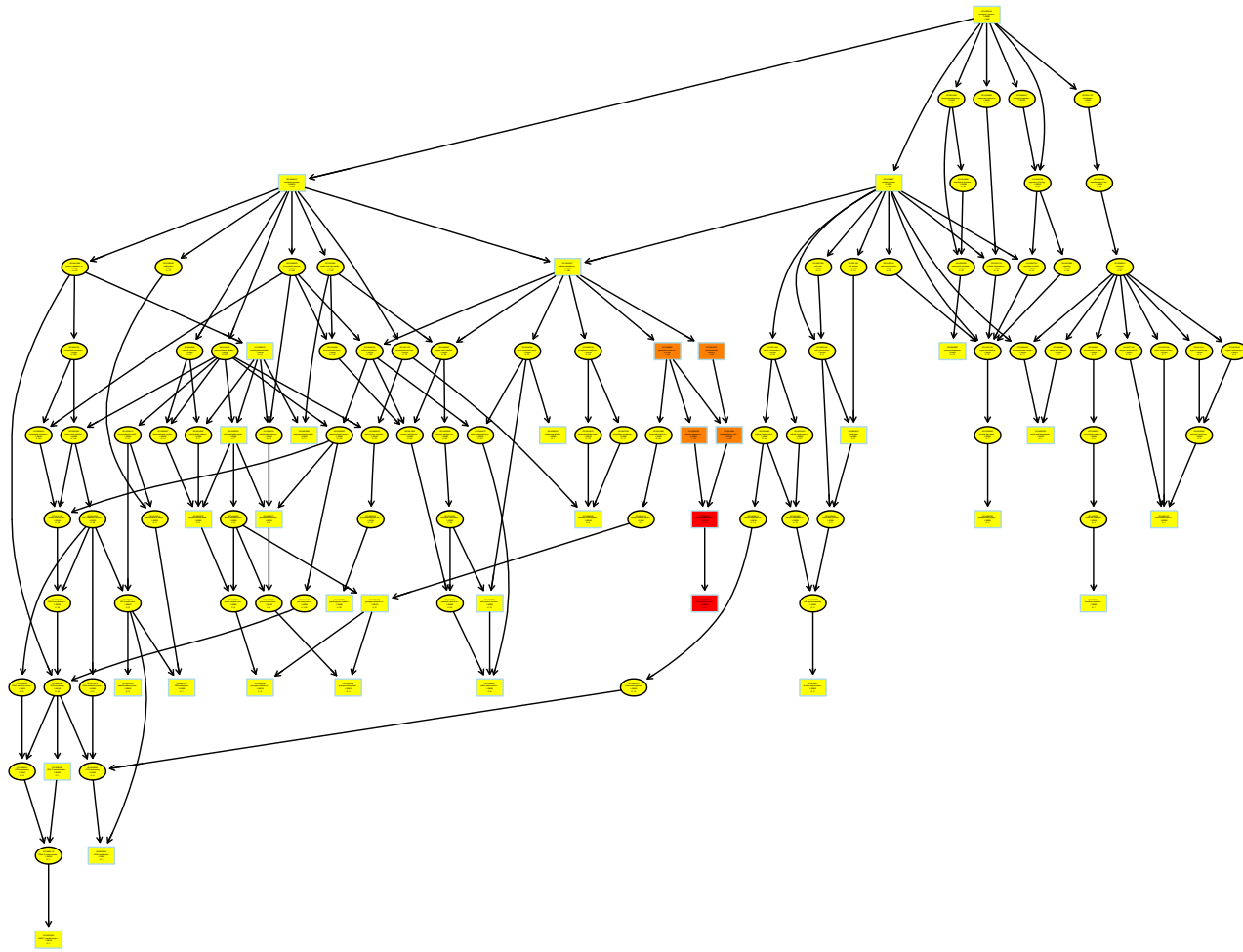


Figure A.7: MEpink GO Enrichment - BP

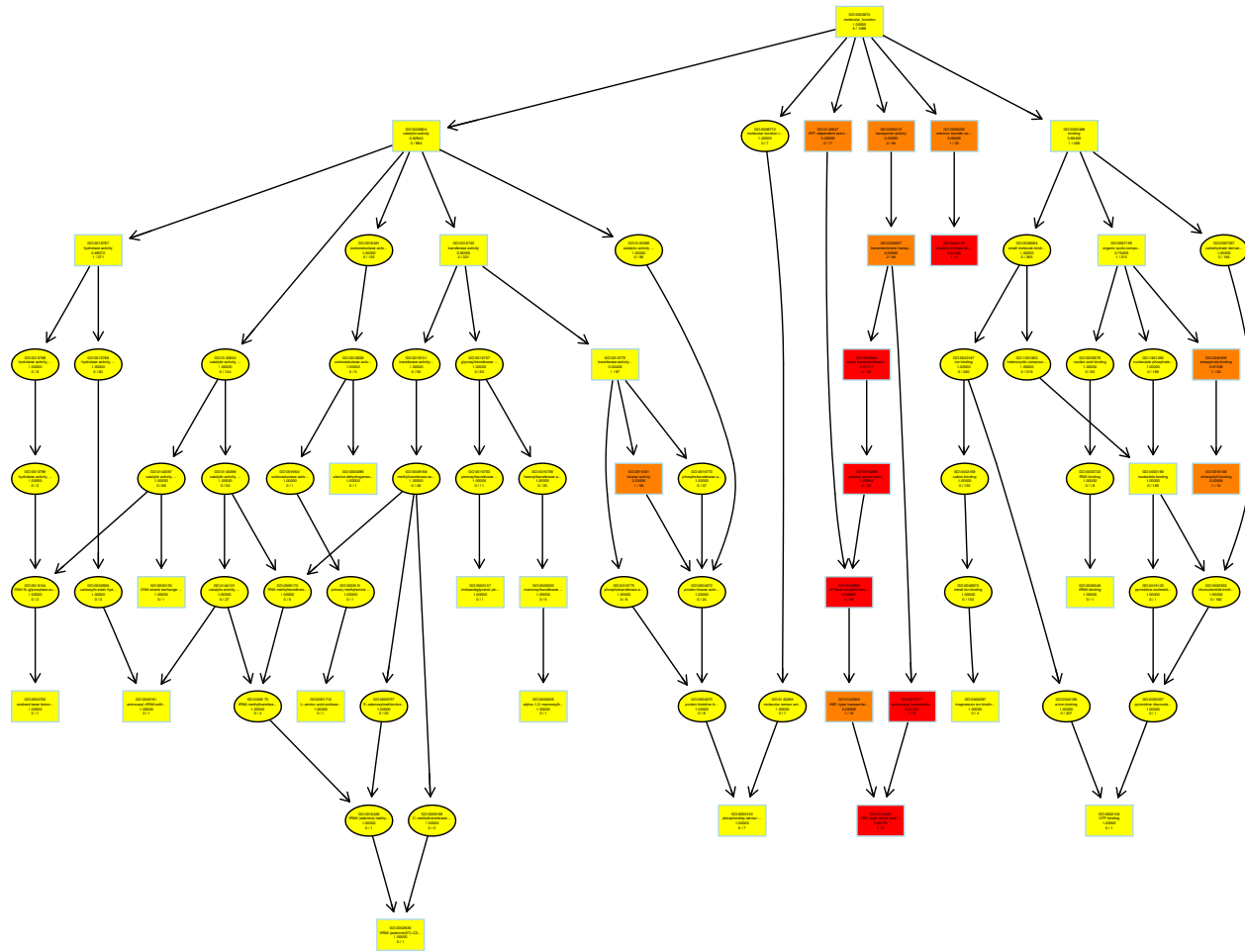


Figure A.9: MEpink GO Enrichment - CC

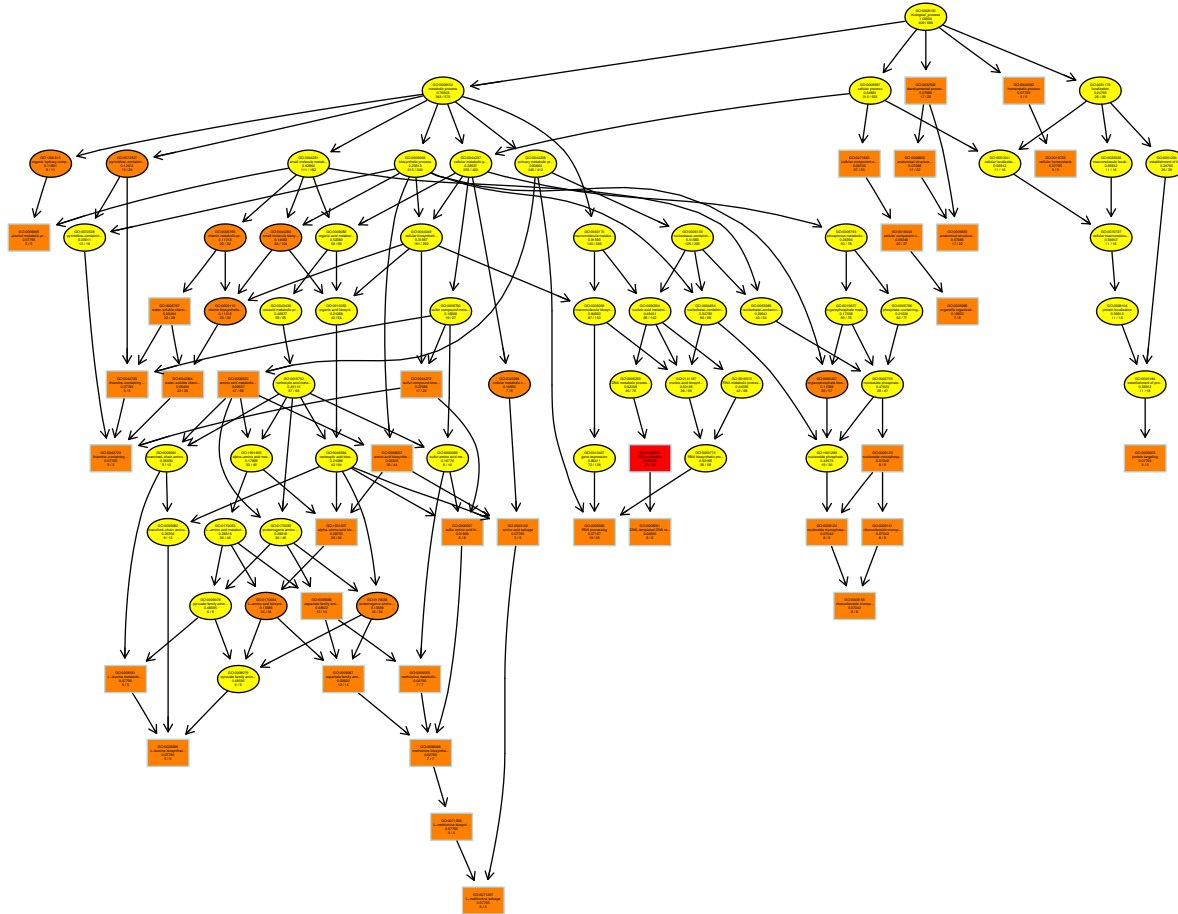


Figure A.10: MEturquoise GO Enrichment - BP

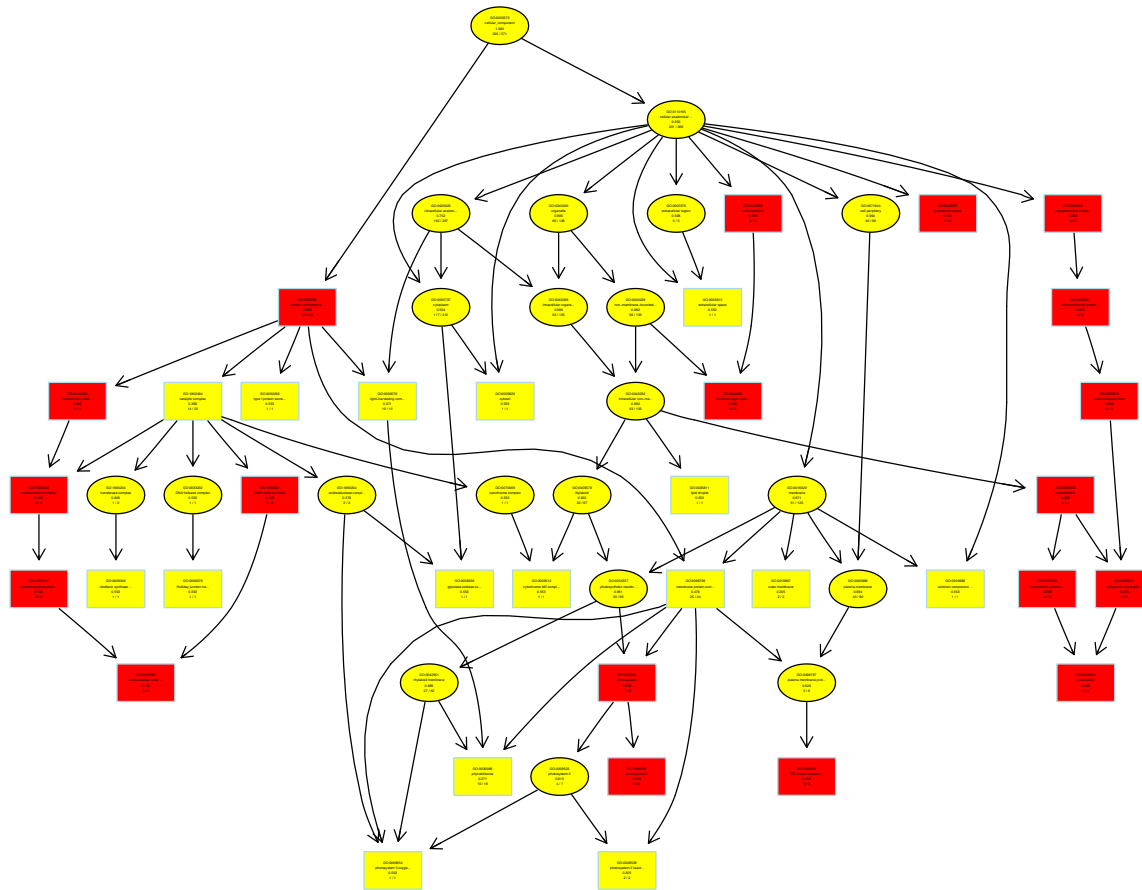


Figure A.11: MEturquoise GO Enrichment - MF

References

1. Mishra, A. *et al.* Role of Cyanobacteria in Rhizospheric Nitrogen Fixation. in *Soil Nitrogen Ecology* (eds. Cruz, C., Vishwakarma, K., Choudhary, D. K. & Varma, A.) 497–519 (Springer International Publishing, Cham, 2021). doi:10.1007/978-3-030-71206-8_25.
2. Yannarell, A. C. & Kent, A. D. Bacteria, Distribution and Community Structure. in *Encyclopedia of Inland Waters* (ed. Likens, G. E.) 201–210 (Academic Press, Oxford, 2009). doi:10.1016/B978-012370626-3.00123-X.
3. Andreeva, N. A., Melnikov, V. V. & Snarskaya, D. D. The Role of Cyanobacteria in Marine Ecosystems. *Russ J Mar Biol* **46**, 154–165 (2020).
4. Schirrmeister, B. E., de Vos, J. M., Antonelli, A. & Bagheri, H. C. Evolution of multicellularity coincided with increased diversification of cyanobacteria and the Great Oxidation Event. *Proc Natl Acad Sci U S A* **110**, 1791–1796 (2013).
5. Sánchez-Baracaldo, P. Origin of marine planktonic cyanobacteria. *Sci Rep* **5**, 17418 (2015).
6. Schirrmeister, B. E., Gugger, M. & Donoghue, P. C. J. Cyanobacteria and the Great Oxidation Event: evidence from genes and fossils. *Palaeontology* **58**, 769–785 (2015).
7. Charpy, L., Casareto, B. E., Langlade, M. J. & Suzuki, Y. Cyanobacteria in Coral Reef Ecosystems: A Review. *Journal of Marine Sciences* **2012**, 259571 (2012).
8. Thajuddin, N. & Subramanian, G. Cyanobacterial biodiversity and potential applications in biotechnology. *Current Science* **89**, 47–57 (2005).
9. Zancan, S., Trevisan, R. & Paoletti, M. G. Soil algae composition under different agroecosystems in North-Eastern Italy. *Agriculture, Ecosystems & Environment* **112**, 1–12 (2006).
10. Singh, J. S., Kumar, A., Rai, A. N. & Singh, D. P. Cyanobacteria: A Precious Bio-resource in Agriculture, Ecosystem, and Environmental Sustainability. *Front. Microbiol.* **7**, (2016).
11. Sciuto, K. & Moro, I. Cyanobacteria: the bright and dark sides of a charming group. *Biodivers Conserv* **24**, 711–738 (2015).
12. Singh, J. S., Kumar, A., Rai, A. N. & Singh, D. P. Cyanobacteria: A Precious Bio-resource in Agriculture, Ecosystem, and Environmental Sustainability. *Front. Microbiol.* **7**, (2016).
13. Nweze, N. Ecological implications and roles of cyanobacteria (cyanophyta) in food security – A review. *Plant Products Research Journal* **13**, (2011).
14. Huisman, J. *et al.* Cyanobacterial blooms. *Nat Rev Microbiol* **16**, 471–483 (2018).
15. Paerl, H. W. & Otten, T. G. Harmful Cyanobacterial Blooms: Causes, Consequences, and Controls. *Microb Ecol* **65**, 995–1010 (2013).

16. Cai, Y., Jiang, J., Zhang, L., Chen, Y. & Gong, Z. Simplification of macrozoobenthic assemblages related to anthropogenic eutrophication and cyanobacterial blooms in two large shallow subtropical lakes in China. *Aquatic Ecosystem Health & Management* **15**, 81–91 (2012).
17. Dong, B., Qin, B., Gao, G. & Cai, X. Submerged macrophyte communities and the controlling factors in large, shallow Lake Taihu (China): Sediment distribution and water depth. *Journal of Great Lakes Research* **40**, 646–655 (2014).
18. Visser, P. M. *et al.* How Increased Carbon Dioxide and Global Warming Stimulate Harmful Cyanobacterial Blooms. *Harmful Algae* **54**, 145–159 (2016).
19. McKee, D. *et al.* Response of freshwater microcosm communities to nutrients, fish, and elevated temperature during winter and summer. *Limnology & Oceanography* **48**, 707–722 (2003).
20. Yang, Z. *et al.* The influence of hydraulic characteristics on algal bloom in three gorges reservoir, China: A combination of cultural experiments and field monitoring. *Water Research* **211**, 118030 (2022).
21. Zou, W. *et al.* Time dependence of chlorophyll a-nutrient relationships in Lake Taihu: drivers and management insights. *Journal of Environmental Management* **306**, 114476 (2022).
22. Bartoli, M. *et al.* Drivers of Cyanobacterial Blooms in a Hypertrophic Lagoon. *Front. Mar. Sci.* **5**, (2018).
23. Beaulieu, M., Pick, F. & Gregory-Eaves, I. Nutrients and water temperature are significant predictors of cyanobacterial biomass in a 1147 lakes data set. *Limnology and Oceanography* **58**, 1736–1746 (2013).
24. Zhang, W. *et al.* The Impact of Cyanobacteria Blooms on the Aquatic Environment and Human Health. *Toxins* **14**, 658 (2022).
25. *Toxic Cyanobacteria in Water: A Guide to Their Public Health Consequences, Monitoring and Management.* (Taylor & Francis, 2021). doi:10.1201/9781003081449.
26. Bláha, L., Babica, P. & Maršálek, B. Toxins produced in cyanobacterial water blooms – toxicity and risks. *Interdiscip Toxicol* **2**, 36–41 (2009).
27. Carmichael, W. W. Health Effects of Toxin-Producing Cyanobacteria: “The CyanoHABs”. *Human and Ecological Risk Assessment: An International Journal* **7**, 1393–1407 (2001).
28. Merel, S. *et al.* State of knowledge and concerns on cyanobacterial blooms and cyanotoxins. *Environment International* **59**, 303–327 (2013).
29. He, X. *et al.* Toxic cyanobacteria and drinking water: Impacts, detection, and treatment. *Harmful Algae* **54**, 174–193 (2016).
30. Havens, K. E. Chapter 33: Cyanobacteria blooms: effects on aquatic ecosystems.

31. Jüttner, F. & Watson, S. B. Biochemical and Ecological Control of Geosmin and 2-Methylisoborneol in Source Waters. *Applied and Environmental Microbiology* **73**, 4395–4406 (2007).
32. Huang, I.-S. & Zimba, P. V. Cyanobacterial bioactive metabolites—A review of their chemistry and biology. *Harmful Algae* **83**, 42–94 (2019).
33. Yu, Q., Liu, Z., Chen, Y., Zhu, D. & Li, N. Modeling the effects of hydrodynamic turbulence on photocompetition between *Microcystis aeruginosa* and *Chlorella vulgaris*. *Ecological Modelling* **370**, 50–58 (2018).
34. Pfeifer, F. Distribution, formation and regulation of gas vesicles. *Nat Rev Microbiol* **10**, 705–715 (2012).
35. Lürling, M., Eshetu, F., Faassen, E. J., Kosten, S. & Huszar, V. L. M. Comparison of cyanobacterial and green algal growth rates at different temperatures. *Freshwater Biology* **58**, 552–559 (2013).
36. Lei, L., Li, C., Peng, L. & Han, B.-P. Competition between toxic and non-toxic *Microcystis aeruginosa* and its ecological implication. *Ecotoxicology* **24**, 1411–1418 (2015).
37. Paerl, H. W. & Paul, V. J. Climate change: Links to global expansion of harmful cyanobacteria. *Water Research* **46**, 1349–1363 (2012).
38. de la Rosa, F., De Troch, M., Gabriela, M. & Marcelo, H. Physiological responses and specific fatty acids composition of *Microcystis aeruginosa* exposed to total solar radiation and increased temperature. *Photochemical & Photobiological Sciences* **20**, 805–821 (2021).
39. de la Rosa, F., De Troch, M., Malanga, G. & Hernando, M. Differential susceptibility to fatty acid and lipid damage in *Microcystis aeruginosa* (cyanobacteria) exposed to elevated temperatures. *Comparative Biochemistry and Physiology Part C: Toxicology & Pharmacology* **235**, 108773 (2020).
40. Gombos, Z., Wada, H. & Murata, N. Unsaturation of fatty acids in membrane lipids enhances tolerance of the cyanobacterium *Synechocystis* PCC6803 to low-temperature photoinhibition. *Proc Natl Acad Sci U S A* **89**, 9959–9963 (1992).
41. Hayakawa, K. *et al.* Fatty acid composition as an indicator of physiological condition of the cyanobacterium *Microcystis aeruginosa*. *Limnology* **3**, 29–35 (2002).
42. Somerville, C. & Browse, J. Plant Lipids: Metabolism, Mutants, and Membranes. *Science* **252**, 80–87 (1991).
43. Basova, M. M. Fatty acid composition of lipids in microalgae. *IJA* **7**, (2005).
44. Tasaka, Y. *et al.* Targeted mutagenesis of acyl-lipid desaturases in *Synechocystis*: evidence for the important roles of polyunsaturated membrane lipids in growth, respiration and photosynthesis. *EMBO J* **15**, 6416–6425 (1996).

45. Somerville, C. Direct tests of the role of membrane lipid composition in low-temperature-induced photoinhibition and chilling sensitivity in plants and cyanobacteria. *Proc Natl Acad Sci U S A* **92**, 6215–6218 (1995).
46. Yano, Y., Nakayama, A., Ishihara, K. & Saito, H. Adaptive Changes in Membrane Lipids of Barophilic Bacteria in Response to Changes in Growth Pressure. *Appl Environ Microbiol* **64**, 479–485 (1998).
47. Williams, J. P., Khan, M. U., Mitchell, K. & Johnson, G. The Effect of Temperature on the Level and Biosynthesis of Unsaturated Fatty Acids in Diacylglycerols of *Brassica napus* Leaves 1. *Plant Physiol* **87**, 904–910 (1988).